Engineering Journal

American Institute of Steel Construction

Second Quarter 2012 Volume 49, No. 2

www.aisc.org

Effect of Washer Placement on Performance of Direct Tension Indicators with Curved Protrusions

DOUGLAS B. CLEARY, WILLIAM T. RIDDELL and CHRISTOPHER J. LACKE

ABSTRACT

A series of tests was performed to evaluate the effect of a hardened washer placed between the turned element and a direct tension indicator (DTI) with curved protrusions. Configurations with ¾-, ⅞- and 1.0-in.-diameter bolts with and without hardened washers were evaluated. Tests were also performed with ¾- and ⅞-in. bolts using a new type of DTI, where the DTI is staked to a nut. The purpose of these tests was to compare the performance of the various configurations, as measured by the number of gaps open at the specified pretension level, the load required to close at least half of the gaps, and the tensile load on the bolts when all or all but one of the gaps in the DTI are closed. When an ASTM A563 grade DH nut was used for a given bolt diameter, some differences were observed to be statistically significant. However, no consistent trends were observed in these differences, and the actual differences were of the same order of magnitude as the load increments used in testing. Therefore, it was concluded that there are no practical differences between the various configurations considered when grade DH nuts are used. However, the DTI did not perform well without a secondary hardened washer when an ASTM A563 Grade C nut was used.

Keywords: direct tension indicators, hardness, washers, bolting.

Tension indicating washers, commonly called direct tension indicators (DTIs), are one of several methods used to achieve or demonstrate adequate bolt pretension when such pretension is required in a bolted connection. Other methods include turn-of-the-nut, calibrated wrenches, and twist-off-type tension-control bolts. ASTM F959-09 states that a direct tension indicator is a "*washer-type element inserted under the bolt head or hardened washer, having the capability of indicating the achievement of a required minimum bolt tension by the degree of direct tension indicator plastic deformation.*" The plastic deformation is indicated by the collapse of protrusions on the face of the tension indicating washer. The extent to which the protrusions have collapsed is determined by the number of gaps between protrusions that a 0.005-in.-thick indicator can be inserted. Direct tension indicators were introduced in the 1960s and their design has evolved over the ensuing years. Previous studies of use of DTIs in structural connections can be found in the literature (Schmeckpeper et al., 1999; Struik et al., 1973).

Douglas B. Cleary, Ph.D., P.E., Associate Professor, Department of Civil and Environmental Engineering, Rowan University, Glassboro, NJ (corresponding author). E-mail: cleary@rowan.edu

William T. Riddell, Ph.D., Associate Professor, Department of Civil and Environmental Engineering, Rowan University, Glassboro, NJ. E-mail: riddell@rowan.edu

Christopher J. Lacke, Ph.D., Associate Professor, Department of Mathematics, Rowan University, Glassboro, NJ. E-mail: lacke@rowan.edu

The Research Council on Structural Connections (RCSC, 2004) *Specification for Structural Joints Using ASTM A325 or A490 Bolts* notes that washers are not required in pretensioned joints and slip-critical joints except in cases of sloping surfaces, oversized or slotted holes, and for certain situations with lower yield strength base material and A490 connectors. In addition, there are requirements for the use of washers under turned elements when using calibrated wrench pretensioning, twist-off-type, tension-control bolt pretensioning and direct tension indicators. As noted in the Commentary of Section 6 of the RCSC specification, "The primary function of washers is to provide a hardened non-galling surface under the turned element, particularly for torque-based pretensioning methods…" Although direct tension indicators are not torque-based, the specification does require an ASTM F436 washer between the direct tension indicator and the turned element.

The original tension indicating washers developed by Cooper and Turner Ltd. required use of hardened washers per the manufacturer's installation instructions because the indicator protrusions in some cases were outside the bearing surface of the bolt or nut. In addition, the protrusions were harder and had a straight-sided shape that could cut or gall the bearing surface of the turned element (Laboratory Testing Inc., 1999). An amendment to ASTM F959 in 1993 ensured that DTIs conforming to that specification would have protrusions that fall within the geometric limits of bolt or nut bearing surfaces. The hardness of current DTIs varies by manufacturer.

Table 1. Matrix of Configurations Considered in Testing						
	Diameter, in.	Type	Surface Finish	Hardened Washer	Nut Grade	Number of Tests
TurnaSure DTI						
Lot 343I76	¾	325	Plain	Yes	DH	30
Lot 343I76	¾	325	Plain	No	DH	30
Lot 783F63-3	⅞	325	Plain	Yes	DH	30
Lot 783F63-3	⅞	325	Plain	No	DH	30
Lot 014B10	1	490	Plain	Yes	DH	30
Lot 014B10	1	490	Plain	No	DH	30
Lot 343I74	¾	325	Plain	No	DH	10
Lot 783F63-3	⅞	325	Plain	No	C	10
TurnAnut DTI						
34TNA6A	¾	325	Plain	No	DH	30
34TNA7A	¾	325	Galvanized	No	DH	30
78TNA6A	⅞	325	Plain	No	DH	30
78TNA6A	⅞	325	Galvanized	No	DH	30

PURPOSE AND SCOPE

The purpose of this study was to evaluate the performance of direct tension indicators with curved protrusions for various washer configurations under controlled laboratory conditions. Tests were performed for ASTM A325 ¾- and ⅞-in.-diameter bolts and ASTM A490 1-in.-diameter bolts with standard ASTM F959 direct tension indicators, with and without ASTM F436 standard hardened washers against ASTM A563 Grade DH nuts. For the ASTM A325 ¾- and ⅞-in. bolts, both galvanized and plain finish proprietary TurnAnut DTIs are also evaluated. The TurnAnut DTI consists of a nut to which a DTI has been attached by staking. An additional test series with ⅞-in.-diameter bolts with ASTM A563 Grade C nuts was also performed. All DTIs were manufactured by TurnaSure, LLC. The test conditions are summarized in Table 1.

CODE REQUIREMENTS FOR DIRECT TENSION INDICATORS

Direct tension indicators must meet the requirements of ASTM F959. Section 7 of the RCSC *Specification* describes the requirements to verify that fastener assemblies

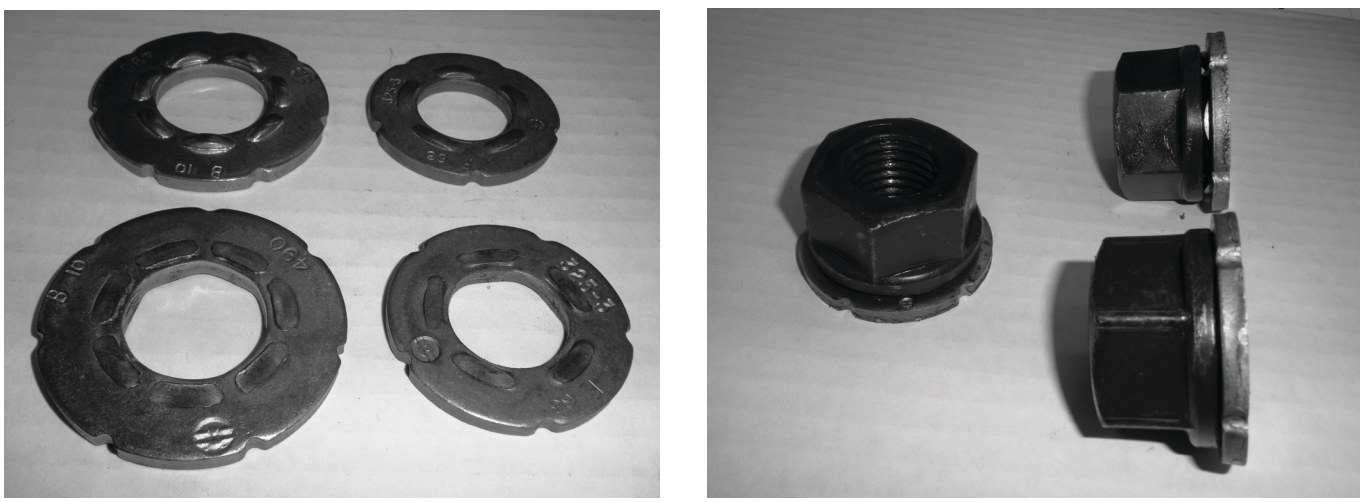

(a) TurnaSure DTI *(b) TurnaSure TurnAnut DTI*

Fig. 1. Views of TurnaSure DTI and TurnAnut DTI. The images show the devices before and after testing.

Table 2. Relevant Tensile Forces for Pretensioned and Slip Critical Bolts						
Nominal Bolt Diameter, d_b, in.	Specified Minimum Bolt Pretension, T_m, kips		1.05 times Specified Minimum Bolt Pretension, kips		Minimum Tensile Capacity, kips	
	ASTM A325 Bolts	ASTM A490 Bolts	ASTM A325 Bolts	ASTM A490 Bolts	ASTM A325 Bolts	ASTM A490 Bolts
¾	28	—	29	—	40	—
⅞	39	—	41	—	56	—
1	—	64	—	67	—	91

and procedures result in the required post tightening performance (RCSC, 2004). The specification calls for the use of a tension calibrator to confirm the performance of the fastener assembly and the pretensioning method to be used by the bolting crew. Section 8 describes installation of fastener components. Section 8.2.4 specifically describes direct-tension-indicator pretensioning.

The RCSC *Specification* calls for a representative sample of fastener assemblies to be tested for each combination of diameter, length, grade and lot to be used. In the snug-tight condition at least half of the DTI gaps must remain open. Testing then proceeds until at least half of the gaps are closed to a 0.005-in. feeler gage. The purpose of the testing is to ascertain that the fastener assembly and fastening procedure develops a pretension equal to or greater than 1.05 times the values specified in Table 8.1 of the RCSC *Specification*. The values from Table 8.1 of interest to this test program, as well as the values scaled by 1.05 used for initial pretensioning in this study are reported in Table 2.

EXPERIMENTAL PROGRAM

The experimental program consisted of tension tests of TurnaSure DTIs (Type 325 ¾ in., ⅞ in. and Type 490 1 in.) and TurnaSure TurnAnut DTIs (Type 325 ¾ in. diameter and ⅞ in. diameter). The devices tested are shown in Figure 1. The tests of DTIs were performed with four configurations, including plain-finish DTIs bearing directly against the face of the nut, plain-finish DTIs bearing against a hardened washer, and both plain and mechanically galvanized TurnAnut DTIs as shown in Figures 1 and 2. In the initial round of testing, 30 assemblies of each configuration were tested with Grade DH nuts. All DTIs of the same size were from the same production lot in the initial round of testing. Two additional series consisted of 10 assembly tests each. The first employed ¾-in.-diameter assemblies with Grade DH nuts and no hardened washer, employing DTIs from a different production lot than was used in the initial round. The second additional series was for ⅞-in. assemblies using the same DTI lot as the initial series against Grade C nuts without hardened washers. The nuts were turned with an electric wrench. A summary of the program was provided in Table 1. The Rockwell hardness measurements for all DTIs, nuts, and washers used are shown in Table 3.

While the nuts were tightened, the tension of the bolts was measured with a Skidmore-Wilhelm bolt tension calibrator with a digital readout. For loading, the bolts were placed through the back of the calibrator and the nut was the turned element. The bolts were initially tensioned to 1.05 times the load specified in Table 8.1 of the RCSC *Specification*. The number of gaps open more than 0.005 in. was determined using a feeler gauge. The bolts were then subjected to incremental increases in tension, with the number of open gaps measured and recorded at each increment, until only one gap remained open. The load increments were on the order of 1 kip to 3 kips. In some instances, the final load increment resulted in all gaps closing. The tension load required to close all or all but one gap was recorded. After loading, it was verified that the nut could be rethreaded for the length of the bolt. The loading plates of the bolt tension calibrator required re-facing at regular intervals. No more than 20 test repetitions were performed on a plate without re-facing. The test equipment is shown in Figure 3.

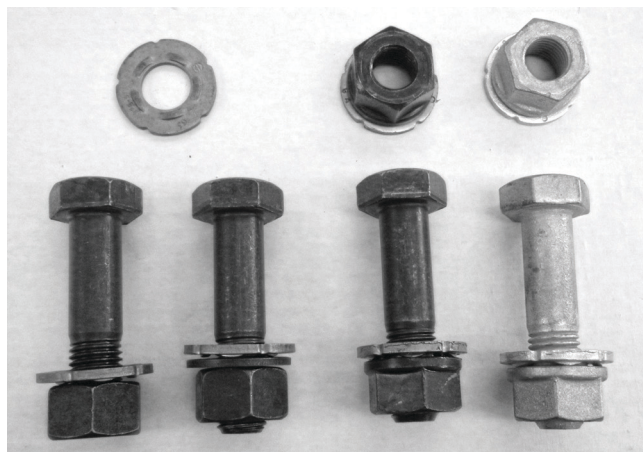

Fig 2. Test configurations from left to right; DTI without washer, DTI with washer, plain TurnAnut DTI, galvanized TurnAnut DTI.

Table 3. Rockwell Hardness of Connection Components (Scale)				
	Diameter, in.	DTI Avg./STD	Washer Avg./STD	Nut Avg./STD
TurnaSure DTI Tests with DH Nuts				
Lot 343I76	¾	87.6/3.09 (B)	39.1/2.48 (C)	30.1/0.42 (C)
Lot 783F63-3	⅞	94.4/1.74 (B)	40.2/1.64 (C)	26.6/1.75 (C)
Lot 014B10	1	83.4/8.91 (B)	42.8/0.84 (C)	28.9/2.53 (C)
Lot 343I74	¾	90.4/3.80 (B)	43.0/2.53 (C)	30.3/2.84 (C)
TurnaSure DTI Tests with C Nuts				
Lot 783F63-3	⅞	94.4/1.74 (B)	Not used	88.37/3.00 (B)

RESULTS

Results of three key load points are reported in this study. The first result reported is the number of gaps open when the pretension in the bolt reaches 1.05 times that specified in Table 8.1 of the RCSC *Specification*. These required pretension values were noted in Table 2. These data are used, similar to pre-installation verification of assemblies as outlined in Section 7 of the RCSC *Specification*, to verify that the required pretension is reached. The required pretension values should be reached prior to half of the DTI gaps closing. The second result reported is the load required to close all or all but one of the DTI gaps. The third finding is the distribution of measured bolt tensions when the DTI indicated that the specified bolt pretension requirements were met (half of the gaps closed).

The average numbers of gaps open at 1.05 times the minimum pretension load and the standard deviation of these results are provided in Table 4. Table 5 provides the distribution of the number of gaps open at this load from tests on ¾-, ⅞- and 1-in.-diameter bolts, respectively. The preload values were 29 kips for ¾-in.-diameter A325 bolts, 41 kips for ⅞-in.-diameter A325 bolts, and 67 kips for 1-in.-diameter A490 bolts.

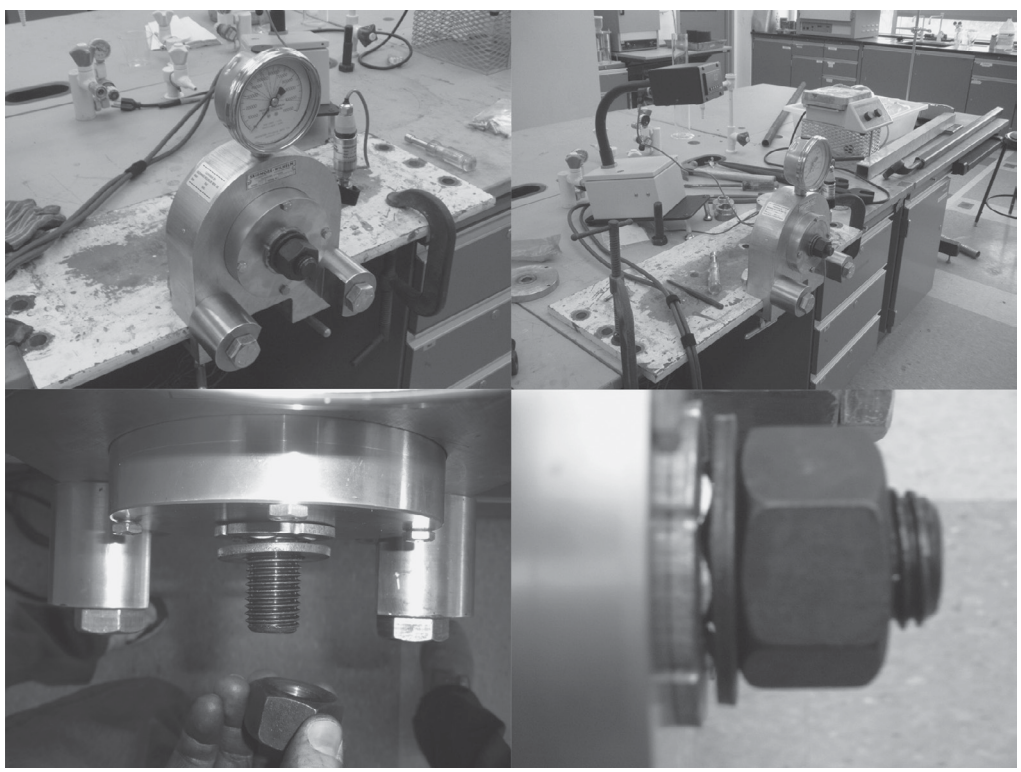

Fig. 3. Test setup.

Table 4. Average Numbers of Gaps Open at 1.05 Times Minimum Pretension Load (Grade DH Nut Unless Otherwise Indicated)		
Assembly (Preload)	**Avg. Number of Gaps Open**	**Standard Deviation**
¾-in. A325 (29 kips)	(5 possible)	
Lot 343I76 without washer	4.10	0.82
Lot 343I76 with washer	3.57	0.73
Lot 343I74 without washer	4.10	1.10
Plain TurnAnut DTI	4.87	0.43
Galvanized TurnAnut DTI	5.00	0.00
⅞-in. A325 (41 kips)	(5 possible)	
Lot 783F63-3 without washer	3.72	0.80
Lot 783F63-3 with washer	3.49	0.85
Lot 783F63-3 without washer (Grade C Nut)	0.91	1.14
Plain TurnAnut DTI	4.93	0.37
Galvanized TurnAnut DTI	4.27	0.74
1-in. A490 (67 kips)	(7 possible)	
Lot 014B10 without washer	6.60	0.89
Lot 014B10 with washer	5.33	1.35

For ¾-in.-diameter assemblies with Grade DH nuts, 39 of 40 tests without a washer and 30 of 30 tests with a backing washer passed simulated pre-installation verification testing. For the ⅞-in.-diameter assemblies with Grade DH nuts, 30 of 30 tests without a washer and 26 of 30 tests with a backing washer passed. All 1-in.-diameter assemblies with DH nuts, with or without a washer, passed the test. All TurnAnut assemblies also passed the simulated pre-installation verification testing. Use of a DTI alone resulted in a higher average number of gaps open at the preload compared to use of a DTI with a hardened washer against the face of the DH nut for all size bolts tested. The TurnAnut DTI, whether plain or galvanized, tended to have the most gaps open at preload and the smallest spread in the results.

The tests of ⅞-in. assemblies with Grade C nuts and without a hardened washer resulted in most of the gaps indicating as closed with the feeler gage at the specified preload (ASTM value times 1.05). This poor performance of the DTI coincided with significant galling of the surface of the Grade C nut.

The average loads required to close all but one or all of the DTI gaps are reported in Table 6. Excluding the results from Grade C nuts, on average, these peak loads are 82 to 96% of the specified minimum tensile capacity of the bolts. Five of 30 tests of galvanized ¾-in. bolts exceeded the minimum specified tensile capacity of the bolt when all or all but one gap was closed. Two tests with ¾-in. galvanized TurnAnut exceeded the minimum specified tensile capacity of the bolt. No other tests exceeded the minimum. Use of a hardened washer against the face of the nut tended to result in a slightly greater spread in the peak load data compared with a DTI directly against the nut face. All nuts could be rethreaded for the length of the bolt after testing, indicating that the bolt did not undergo significant plastic deformation.

Cumulative density functions of the loads measured when at least half of the DTI gaps were first observed to be closed are shown in Figures 4, 5 and 6 for ¾-, ⅞- and 1-in.-diameter assemblies with Grade DH nuts, respectively. These figures indicate the spread in pretension measured under the acceptance condition. The minimum pretension had been developed under this condition for all assemblies tested. The spread of the results was smaller for tests without a hardened washer for ¾- and ⅞-in. assemblies and larger for the 1-in. assemblies. The TurnAnut produced higher pretension than the assemblies in which the washer, DTI or both were free to "float" while the assembly was tightened.

The requirement to place a hardened washer between the turned element and a DTI was because of the potential for DTIs to gall the underside of the nut or bolt head, resulting in incorrect indication of tension. Following this testing, a selection of washers and nuts were inspected both visually and with a profilometer. Visual observation shows that the DTI produced limited polishing of the washer or Grade DH nuts in a ring described by the indicators' protrusions. The profilometer measurements showed no evidence of surface galling. However, the surface of the polished region was

Table 5. Distribution of Gaps Open at 1.05 Times Minimum Pretension Load (Grade DH Nut Unless Otherwise Indicated)						
Assembly (Preload)	**Percentage of Tests with Number of Gaps Open**					
¾-in. A325 (29 kips)	**5**	**4**	**3**	**2**	**1**	**0**
Lot 343I76 without washer ($n = 30$)	38	34	28	0	0	0
Lot 343I76 with washer ($n = 30$)	13	30	57	0	0	0
Lot 343I74 without washer ($n = 10$)	50	20	20	10	0	0
Plain TurnAnut DTI ($n = 30$)	90	7	3	0	0	0
Galvanized TurnAnut DTI ($n = 30$)	100	0	0	0	0	0
⅞-in. A325 (41 kips)	**5**	**4**	**3**	**2**	**1**	**0**
Lot 783F63-3 without washer ($n = 30$)	21	31	48	0	0	0
Lot 783F63-3 with washer ($n = 30$)	13	32	42	13	0	0
Lot 783F63-3 without washer (Grade C nut) ($n = 10$)	0	0	20	30	10	40
Plain TurnAnut DTI ($n = 30$)	97	0	3	0	0	0
Galvanized TurnAnut DTI ($n = 30$)	43	40	17	0	0	0
1-in. A490 (67 kips)	**7**	**6**	**5**	**4**	**3**	**2**
Lot 014B10 without washer ($n = 30$)	80	6	7	7	0	0
Lot 014B10 with washer ($n = 30$)	37	0	23	40	0	0

noticeably smoother, possibly due to limited removal of mill scale as the nut or washer rotated relative to the DTI protrusions. This result was expected because the DTI material is softer than that of either the washer or Grade DH nut. As noted previously however, there was significant galling of the Grade C nuts when the DTI was used without a hardened washer.

ANALYSIS AND DISCUSSION

The test program clearly shows that the tested DTI cannot be used without a hardened washer between it and a Grade C nut. However, in the case of a hardened nut, the extra washer does not appear to be necessary. For the assemblies tested with a sample size of 30 tests, independent sample *t*-test analyses were performed to determine if there were statistically significant differences in the average loads required to close all but one or all of the gaps of the DTI to refusal of the 0.005-in. feeler gauge. The Shapiro-Wilk test was used to assess the validity of the normality condition ($\alpha = 0.2$). Non-pooled *t*-tests were used when the larger standard deviation was more than twice the value of the smaller standard deviation. Results of this analysis, which are exclusive to testing with Grade DH nuts, were:

- The differences in the measured average peak loads were not statistically significant when comparing the "with-washer" configuration to the TurnAnut DTI configuration for plain A325 ¾- or ⅞-in.-diameter bolts.

- The differences in the measured average peak loads were statistically significant when comparing the "with-washer" configuration to the TurnAnut DTI configuration for galvanized A325 ¾-in. bolts. However, the difference was not statistically significant when comparing the "with-washer" configuration

Table 6. Average Loads Required to Close All But One or All of the DTI Gaps (Grade DH Nuts Only)			
Assembly (Minimum Specified Tensile Strength)	**Avg. Peak Load (kips)**	**Standard Deviation (kips)**	**Percent of Minimum Specified Tensile Strength**
¾-in. A325 (40 kips)			
Lot 343I76 without washer	35.1	1.03	88
Lot 343I76 with washer	35.9	1.74	90
Lot 343I74 without washer	34.6	2.27	87
Plain TurnAnut DTI	35.3	1.50	88
Galvanized TurnAnut DTI	38.2	1.60	96
⅞-in. A325 (56 kips)			
Lot 783F63 without washer	45.8	1.42	82
Lot 783F63 with washer	47.4	2.46	85
Plain TurnAnut DTI	48.2	0.89	86
Galvanized TurnAnut DTI	47.2	1.65	84
1-in. A490 (91 kips)			
Lot 014B10 without washer	80.0	3.47	88
Lot 014B10 with washer	77.4	3.92	85

to galvanized A325 ⅞-in.-diameter TurnAnut DTIs. The "with-washer" configuration with ¾-in.-diameter bolts resulted in lower peak bolt tension required to close one or all gaps than was required with the galvanized TurnAnut DTI.

- The differences in the measured average peak loads were statistically significant when comparing the "with-washer" condition to the "without-washer" configuration for all sizes tested. However, the differences were not in the same direction for all sizes. For A325 ¾-in. or ⅞-in.-diameter bolts, the force required to close one or all of the gaps to less than 0.005 in. was higher for the hardened washer configuration. The trend was reversed in the 1-in.-diameter A490 bolts.

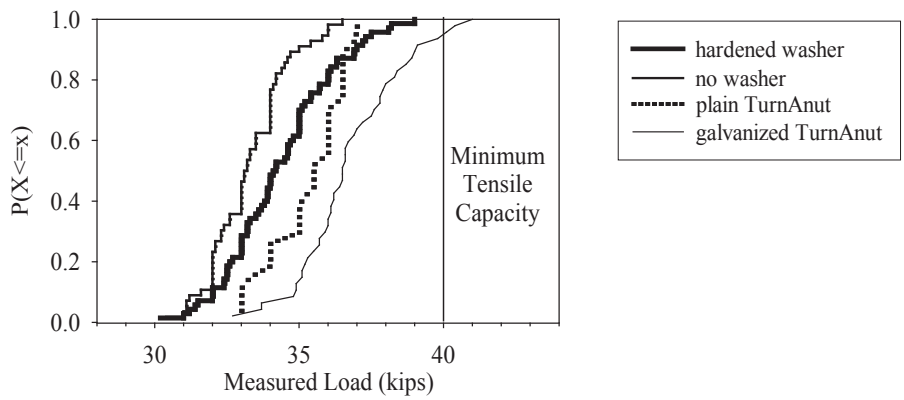

Fig. 4. Cumulative density function of loads required to close half of the gaps, ¾-in.-diameter A325 bolts (minimum pretension is 28 kips and minimum tensile strength is 40 kips).

While the analysis performed indicates there are statistically significant differences in some of the measured results, there was not a consistent trend in these differences. In addition, these statistical findings must be considered in light of the test program itself. The peak loads recorded were those required to close all but one or all of the gaps between the DTI and washer or bolt. This was because in some instances the load increment applied to the bolt resulted in enough gaps closing to bypass the one-gap-closed condition. In addition, the load increments typically ranged from 0.4 kip to 1.5 kips. Therefore, the load increments are equal to or of the same magnitude as the measured differences in peak load values. Given these considerations, these results should not be extended beyond stating that the comparable behavior was achieved with all of the bolt/DTI/washer/nut configurations considered.

SUMMARY AND CONCLUSIONS

Tests of bolt assemblies that involved direct tension indicators with curved protrusions were performed to evaluate the effect of nut and washer configuration on pretension loads achieved. Test configurations included plain DTIs against the face of the nut, DTI's and hardened washer against the face of the nut, and plain and mechanically galvanized

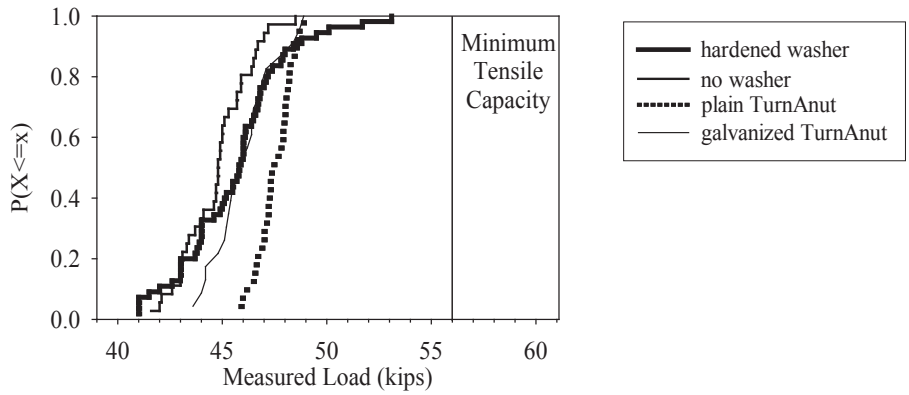

Fig. 5. Cumulative density function of loads required to close half of the gaps, ⅞-in. A325 bolts (minimum pretension is 39 kips and minimum tensile strength is 56 kips).

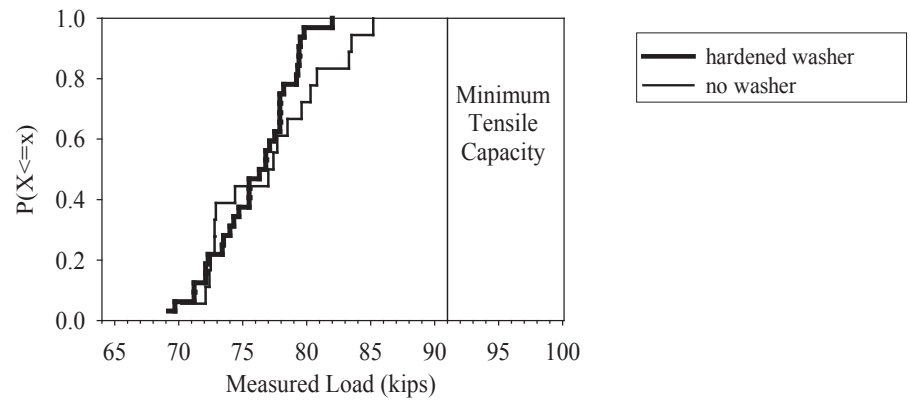

Fig. 6. Cumulative density function of loads required to close half of the gaps, 1-in. A490 bolts (minimum pretension is 64 kips and minimum tensile strength is 91 kips).

TurnaSure TurnAnut DTIs. For all tests, the nut was the turned element. It was found that a hardened washer is necessary if a DTI is used with a Grade C nut. However, it was found that when a Grade DH nut was used, the assembly performed just as well with or without the hardened washer placed between the DTI and the nut.

Additional findings specific to Grade DH nuts were

- Use of a DTI alone resulted in a higher average number of gaps open at the preload compared to use of a DTI with a hardened washer against the face of the nut for all size bolts tested, even when such DTIs were from the same production lot.
- The TurnAnut DTI, whether plain or galvanized, tended to have the most gaps open at preload and the smallest spread in the results.
- In simulated pre-installation verification testing, similar performance of DTI assemblies with or without a hardened washer was observed with a small percentage of assemblies not passing the testing.
- Use of a hardened washer against the face of the nut tended to result in a slightly greater spread in the peak load data compared with a DTI directly against the nut face. For the condition of half of the gaps closed the finding was similar for ¾- and ⅞-in.-diameter assemblies but opposite with 1-in.-diameter assemblies.
- In some cases statistically significant differences were measured for the average tensile loads required to close all but one or all of the gaps to less than 0.005 in. However, the trends were not consistently in the same direction and the differences in the means were less than or comparable to the load increments being applied during the testing.

Based on the results of this test program, it is concluded that the use of direct tension indicators with curved protrusions with or without hardened washers against the turned element for ASTM A325 ¾- and ⅞-in.-diameter bolts and ASTM A490 1-in.-diameter bolts results in comparable performance in providing the required bolt pretension if a Grade DH or harder nut is used. In addition, the presence or absence of the hardened washer made no difference in the performance of the direct tension indicators at the load levels required to close all but one or all of the gaps. The staking of a direct tension indicator to a nut to produce the TurnAnut DTI configuration with either plain or galvanized surfaces also resulted in behavior comparable to a DTI with and without a hardened washer against the turned element. However, the testing does not support elimination of the hardened washer for softer grades of nuts.

ACKNOWLEDGMENTS

The work presented was sponsored by Turnasure, LLC. The views presented do not necessarily represent those of the project sponsors. The testing was carried out by undergraduate research assistants Mr. Matt Janas and Mr. Ryan Headley with assistance from Mr. Charles Linderman.

REFERENCES

ASTM (2007), *ASTM A563-07a Standard Specification for Carbon and Alloy Steel Nuts,* American Society for Testing and Materials, American Society for Testing and Materials, West Conshohoken, PA.

ASTM (2009), *ASTM F436-09 Standard Specification for Hardened Steel Washers*, American Society for Testing and Materials, West Conshohoken, PA.

ASTM (2009), *ASTM A325-09 Standard Specification for Structural Bolts, Steel, Heat Treated,* 120/1*05 ksi Minimum Tensile Strength*, American Society for Testing and Materials, West Conshohoken, PA.

ASTM (2009), *ASTM A490-09 Standard Specification for Heat Treated Steel Structural Bolts, 150 ksi Minimum Tensile Strength*, American Society for Testing and Materials, West Conshohoken, PA.

ASTM (2009), *ASTM F959-09 Standard Specification for Compressible-Washer-Type Direct Tension Indicators for Use with Structural Fasteners*, American Society for Testing and Materials, West Conshohoken, PA.

Laboratory Testing Inc. (1999), "Influence of Curved Protrusion Design on Installation of Structural Direct Tension Indicators (DTIs)—Curved Protrusion DTIs Used Under the Turned Element," http://turnasure.com/pdf/reports/Curved%20Protrusion%20DTIs.pdf (viewed June 21, 2009).

RCSC (2004), *Specification for Structural Joints Using ASTM A325 or A490 Bolts*, Research Council for Structural Connections, Chicago, IL.

Schmeckpeper, E.R., Nielsen, R.J. and Genry, G. (1999), "The Effects of Over-Compressing AST F959 Direct Tension Indicators on A325 Bolts Used in Shear Connections," *Engineering Journal*, AISC, Vol. 36, No. 1, pp. 55–70.

Struik, J.H.A., Oyeledun, A.O. and Fisher, J.W. (1973), "Bolt Tension Control with a Direct Tension Indicator," *Engineering Journal*, AISC, Vol. 10, No. 1, pp. 1–5.

A Simplified Approach for Evaluating Second-Order Effects in Low-Rise Steel-Framed Buildings

SOUHAIL ELHOUAR and YASSER KHODAIR

ABSTRACT

Consideration of second-order effects is one of the most involved tasks in the analysis and design of steel-framed buildings. More specifically, the evaluation of amplified moments due to frame-level second-order effects is a very time consuming task because, depending on the method used, it may require an additional first-order analysis or the introduction of additional notional loads for each considered load case. Although the use of such methods may not present a problem when the design process is fully automated, hand calculations can be quite complicated for checking the results of a computer-generated design or for designing a small structure in which second-order effects may not even be significant enough to affect the selection of member sizes. This paper presents a simplified approach for the incorporation of second-order effects in the design of low-rise steel-framed structures. The development of this approach involved the design and analysis of a number of systems with various numbers of bays, floors and beam-span to floor-height ratios and included a thorough investigation of the effect of moment amplification on final member sizes. To facilitate this task, a spreadsheet application was developed to automate the design of a typical low-rise steel frame under given loading conditions. A parametric study was then performed to understand the effect of the various design parameters on member-level and frame-level second-order forces and moments. This led to the development of the simplified design approach proposed in this paper.

Keywords: second-order effects, P-delta, load amplification, low-rise buildings, simplified procedure.

INTRODUCTION

Traditional structural analysis methods are based on the assumption that the deformation of a member does not affect its internal load or stress distributions. This is usually referred to as first-order analysis. However, for flexible structural systems, the extra forces or stresses induced by deformations may be quite significant and cannot be ignored. Steel frames are such structures, and the 2010 AISC *Specification for Structural Steel Buildings* states that second-order effects should be considered in the design of frames. The *Specification* provides several different approaches for doing so, including the approximate second-order analysis method presented in Appendix 8 of the 2010 AISC *Specification*.

Nevertheless, there is sufficient evidence from practice that the design of low-rise buildings may not be greatly affected by second-order effects. Carter et al. (2000) note that "most building structures in the United States are not taller than four stories and the actual increase in moments due to deformations of the frame is in many practical cases negligible." Carter et al. also state that there are cases where the consideration of the effect of these deformations can be important. They further make the case for the need for a simplification of specification requirements for the consideration of second-order effects. This paper presents the results of an investigation that was carried out to accomplish this goal.

Souhail Elhouar, Ph.D., P.E., Associate Professor, Department of Civil Engineering and Construction, Bradley University, Peoria, IL (corresponding author). E-mail: selhouar@bradley.edu

Yasser Khodair, Ph.D., P.E., Assistant Professor, Department of Civil Engineering and Construction, Bradley University, Peoria, IL. E-mail: ykhodair@bradley.edu

REVIEW OF LITERATURE

The analysis and design of steel buildings based on second-order methods can be cumbersome. Ordinary structural analysis methods that do not take the displaced geometry of a member into consideration are identified as first-order methods. Second-order methods are used to find the deflections and secondary moments that could be significant depending on the type of structure and its geometry, loading and support conditions. Several methods have been developed to estimate the second-order effects in steel buildings. Carter and Geschwindner (2008) compared three approaches presented in the 2005 AISC *Specification* and a fourth approach presented in the 13th edition AISC *Steel Construction Manual*:

1. Second-order analysis method (AISC 2005a, Section C2.2a).
2. First-order analysis method (AISC 2005a, Section C2.2b)
3. Direct analysis method (AISC 2005a, Appendix 7)

4. Simplified method (AISC 2005b, p. 2-12 and the AISC *Basic Design Values* cards)

The authors used two simple unbraced frames to compare these methods. The first frame is a one-bay frame that has a rigid roof element spanning between a flagpole column and a leaning column. Drift limitations were not specified for this frame, resulting in a higher ratio of second-order drift to first-order drift, which illustrates the requirements needed for each method to calculate *K*-factors, notional loads, and required and available strengths. The second frame is a three-bay frame that has rigid roof elements spanning between two flagpole columns and two leaning columns. The drift limit for this frame was specified to be *L*/400 to illustrate the simplification that specifying a drift limit can provide on the analysis of each method. The authors compared these four methods based on the result of the beam-column interaction equation. It was found that the direct analysis method calculates the highest strength, while the simplified method calculates the lowest strength. However, the results for the three-bay frame showed that the values of the interaction formula produced very close results, and there are no significant differences between them. The authors concluded that if conservative assumptions are acceptable, the simplified method would be the simplest approach to use, especially if the drift limit is such that *K* can be taken equal to 1. Furthermore, second-order effects and leaning columns have a significant impact on strength requirements, but usual drift limits such as *L*/400 sometimes can result in framing that requires no increase in member size for strength.

Eroz et al. (2008) addressed the consideration of partial base fixity using the direct analysis method (DM). The authors developed a refined model of the column base moment-rotation response using an adaptation of the component method (CM) of Eurocode 3 plus a representation of the foundation stiffness. Furthermore, the authors applied an extension of the DM for frames containing web-tapered members. An example clear-span gable frame is checked using several models of its nominally simple four-bolt base detail: ideally pinned, elastic based on $G = 10$ from the AISC sidesway-uninhibited alignment chart, and elastic-perfectly plastic using the component method (CM). It was also shown that the member strength unity checks and the frame deflections obtained by modeling of the column bases as elastic based on $G = 10$ are accurate compared to the refined base model. It is found that the contribution of the significant initial stiffness of typical bases to the overall frame response is limited by the connection strength.

Becker (2008) reviewed a rigid frame that Chief Buildings designed using allowable stress design per the 1989 AISC *Specification* with the effective length method. This design was compared with an analysis of this structure using the direct analysis method from Appendix 7 of the 2005 AISC *Specification* using both ASD and LRFD load combinations. This comparison showed that various load combinations and methods of applying floor live loads can have very dynamic effects on the amplification of moments due to the P-δ effects. Moreover, the author realized that slight variations in the frame configuration and modeling can greatly affect the P-δ moments.

Surovek and Ziemian (2005) presented an overview of known frame analysis methods and described the connection between these methods and specification based approaches for assessment of frame stability. The authors discussed the effectiveness of the direct analysis method in achieving greater simplification in analysis and design checks. The authors discussed three design approaches for assessment of frame stability:

1. The AISC LRFD effective-length-based assessment (AISC, 1999)
2. The direct analysis method
3. An advanced analysis method

The paper highlighted the main differences between the three approaches pertaining to the level of analysis required, the method of accounting for the effects of member inelasticity, and the means for including the effects of geometric imperfections due to fabrication and erection tolerances. Three design approaches were also compared using a design example that included an 11-bay single-story frame. The study concluded that the direct analysis approach produces an accurate representation of the actual behavior of the framing system as it accounts for the effects of member inelasticity and frame imperfections in the assessment of both member and system strengths. This approach is implemented in design offices and is used in the analysis of braced frames, moment frames and mixed systems through the use of commercially available software. This reduces the need for using approximate methods such as those using the effective length factor concept.

Kim and Choi (2005) developed a practical second-order inelastic analysis of three-dimensional steel frames subject to distributed loading. The authors utilized stability functions to account for second-order effects associated with P-δ and P-Δ. The Column Research Council (CRC) tangent modulus concept is used to account for gradual yielding due to residual stresses. The degradation from elastic to zero stiffness associated with development of a hinge was represented by a softening plastic hinge model. In their proposed analysis, the authors represent a member by two elements and three nodal points. A plastic hinge location can be captured in the analysis as the internal nodal point traces the maximum moment location at each load step. Maximum moments and load–displacement relationships predicted by the proposed analysis compared well with those given by other approaches.

Chen and Wang (1999) proposed a new moment amplification factor B_1* for calculating the P-δ effect in the design of steel beam-columns. The main purpose of the new moment amplification factor was to replace the B_1 factor of the 1993 AISC LRFD *Specification* in order to account for inaccuracies in predicting P-δ effects especially when the member is subjected to large magnitudes of axial load. Moreover, the researchers have conducted parametric studies to evaluate the accuracy of the proposed moment amplification factor and compare it with that from theoretical analysis and current design specification. The researchers stated that the new factor is more precise in predicting P-δ effects when compared with the current design specification.

Sohal and Syed (1992) developed an inelastic amplification factor (IAF) to account for the inaccuracies associated with using the elastic amplification factor that was proposed in the literature. The elastic amplification factor provided a good estimation of the amplified moment only for members with very high slenderness that fail by elastic buckling. However, members with intermediate slenderness, especially those with high shape factors, will fail by inelastic buckling. Design interaction equations developed with the LRFD B_1 factor and the inelastic amplification factor proposed by the authors were compared with numerical inelastic strengths of beam columns. The authors concluded that:

1. The inelastic amplification factor (IAF) is higher than the elastic amplification factor for all studied cases.

2. The IAF increases with decreasing slenderness ratios for any given value of applied load to critical load P/P_{cr}.

3. The effects of residual stresses and initial out-of-straightness increase the IAF.

4. The use of the IAF in the present LRFD interaction for beam-columns bending about their weak axes results in an over-conservative prediction of the strength of most beam-columns.

Duan and Chen (1989) developed a unified design interaction equation for braced steel beam columns subjected to compression combined with biaxial bending. The proposed interaction equation satisfies both strength and stability criteria. A comparison between the proposed design equation, as well as the AISC equations, with the exact inelastic solutions of I-shaped beam-columns and with the results obtained from 81 full-scale tests of biaxially loaded I-shaped beam-columns was made. The authors concluded that the proposed formula is simple in format, has a smooth transition from the pure bending case to the pure axial load case, and is valid for long and short members. They also indicated that the proposed formula is only valid for I-sections as formula parameters will be different for other sections.

This literature survey showed that extensive research has been conducted in the design and analysis of steel-framed buildings to account for second-order effects, but none of this research dealt specifically with low-rise buildings or tried to come up with a simplified approach for their design

DEVELOPMENT OF THE PROPOSED SIMPLIFIED DESIGN METHOD

For structures designed on the basis of first-order elastic analysis, the 2010 AISC *Specification* provides an approximate method to account for second-order effects. This method involves the application of moment and axial force amplification factors to results that are obtained using first-order analyses. The amplified effects are given by the following 2010 AISC *Specification* equations:

$$M_r = B_1 M_{nt} + B_2 M_{lt} \qquad \text{(AISC 2010, Eq. A-8-1)}$$

$$P_r = P_{nt} + B_2 P_{lt} \qquad \text{(AISC 2010, Eq. A-8-2)}$$

In these equations, M_r and P_r are the second-order moment and axial force to be used in member verification, M_{nt} and P_{nt} are the first-order moment and axial force obtained using LRFD or ASD load combinations assuming no lateral translation of the frame, and M_{lt} and P_{lt} are the first-order moment and axial force that are due to lateral reactions from those same LRFD or ASD load combinations but assuming lateral translation of the frame is possible. The factor B_1 is used to approximate second-order effects at the member level (P-δ effects), and the factor B_2, which is only applicable to unbraced frames, is used to account for second-order effects at the frame level (P-Δ effects). Two approaches can be used to compute B_2: one is based on the elastic story sidesway buckling resistance, and one is based on limiting interstory drift. The procedure being proposed herein is based on the approach that uses the elastic story buckling resistance.

One of the easiest ways the process can be simplified is to eliminate the need for the two analyses that are required to compute the coefficients B_1 and B_2. This would be straightforward for structures with a given set of characteristics if it is known that one of the effects is dominant over the other. This is because, for such structures, amplified load effects may be directly related back to total load effects without having to distinguish between member-level and frame-level amplification since the amplification is mainly coming from one source. Based on this observation, and since the objective is to come up with a simplified procedure for low-rise building structures, it was decided to examine amplification factors for a number of these structures to determine if either of the effects is dominant. This required that a large number of low-rise structures be designed to obtain enough data to analyze and base a possible new procedure upon. These

systems were one to four floors high and one to four bays wide. For each system bay, length was set to 22.5, 25, 27.5, 30 or 32.5 ft, whereas floor height was kept at 15 ft. This variety in frame aspect ratios ensures an adequate representation of building geometries. The frame spacing for each system was taken as 20, 24, 30 or 40 ft and a 120-ft total building width was assumed. The unbraced length of roof beams was set to a 5-ft assumed typical roof joist spacing, and floor beams were assumed to be fully braced by supported slabs. Each column was assumed to be pinned at the base and braced at one-third height (i.e., at 5-ft intervals) with respect to its weak axis to ensure that strong axis buckling controls the design of all the columns. This will ensure that any design parameters that are to be obtained from this procedure will be applicable to the column under consideration irrespective of its lateral bracing configuration.

The gravity loads applied to each system consisted of an 80-psf dead load, a 50-psf live load, and a 25- and 20-psf roof dead and live load, respectively. Lateral loads consisted of wind and seismic and were based on input data for the Peoria, Illinois, area (wind speed of 90 miles per hour, a short period mapped spectral response acceleration of 17.5% g, and a long period mapped spectral response acceleration of 7.8% g). A specific location is being mentioned only to have a point of reference for initial design load determination; any other location could have served the purpose of this investigation. Figure 1 shows the elevation drawing of a typical frame and loads. Considering that 320 frames needed to be designed, a spreadsheet application was developed to automate the design process and complete the task in a timely and efficient manner. This application accepts as input the number of floors, number of bays, first floor height, typical beam span-to-floor height ratio, preferred beam and column nominal depths, and typical loads. It then goes on to generate the structural model and loads and then finds the lightest hot-rolled section for each structural member. The development of a special spreadsheet application for this project was judged to be more efficient than using available structural analysis and design software for the following reasons:

1. The structural model generation and load application processes can be automated, leading to a minimum amount of data input being required for each run.

2. A better control of the design process in terms of member sizes and groupings can be achieved.

3. The ability exists to extract any intermediate data that might be deemed useful for the parametric study. Most of these data are impossible to get from currently available commercial software.

Upon completing each design, member section, member level and position, ϕP_n, ϕM_n, P_{nt}, P_{lt}, M_{nt}, M_{lt}, B_1, B_2 and the interaction ratio were stored for each member in the system. The results of the designs of all the systems were then combined in a single worksheet that was used for the parametric analysis. Figure 2 shows a partial screen capture of the results worksheet of the spreadsheet application for a typical two-bay, two-floor system.

PARAMETRIC ANALYSIS

A perusal of the results from the performed analyses showed a clear dominance of frame-level moment and axial force magnification for the types of structures under consideration because the values of B_1 for all members were around 1.0, while values of B_2 varied from 1.01 to 1.29. This means that it may be possible to directly relate amplified moments and forces to those obtained from a first-order analysis using one single amplification coefficient. For a system that was designed using the B_1/B_2 amplification method, single amplification coefficients for axial load and moment can be defined as $B_P = P_u/(P_{nt} + P_{lt})$ and $B_M = M_u/(M_{nt} + M_{lt})$, respectively.

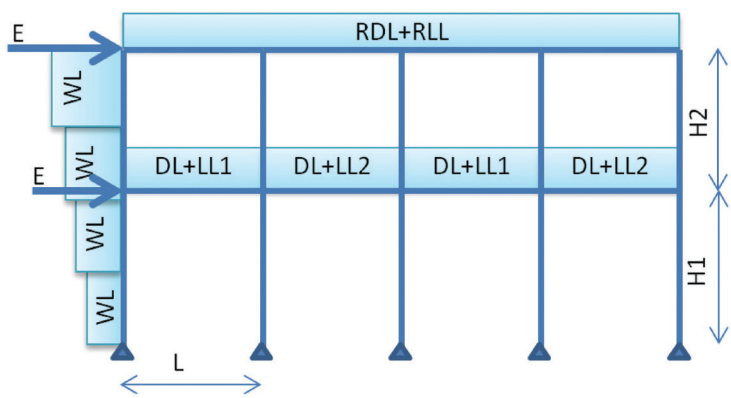

Fig. 1. Typical design frame geometry and loading.

B_P is an axial force magnification coefficient and B_M is a bending moment amplification coefficient. These newly defined coefficients were then computed for all the columns that were designed in the selected systems, and their variation with various design parameters (such as the number of floors, number of bays, bay length, member level and member position) were examined. Member level refers to the floor the column belongs to, and member position refers to the position of the column within the floor, i.e., exterior or interior. In general, the parametric analysis showed that axial force and bending moment magnification was mainly affected by the level of the member and the number of floors in a system and, to a lesser extent, by the number of bays. Member position within the frame seems to have some effect on the moment magnification coefficient B_M but not as much on the axial force magnification coefficient B_P. Values of B_M were observed to be 2.2 to 9.5% higher for interior columns than those for exterior columns depending on the number of floors, number of bays and bay width to frame height ratio.

Figure 3 shows a typical variation of the axial force magnification coefficient B_P, and Figure 4 shows a typical variation of the bending moment magnification coefficient B_M with member level. These coefficients are noticeably higher for first floor columns than they are for upper level columns. Moreover, it is interesting to note that the B_P and B_M coefficients are higher for columns at the third level than they are for those at the second level. This can be explained by the adopted design approach because a change in column size was set to occur after every two floors. As a result, the columns at the first and third levels are the ones governing the design and the columns at the second and fourth levels ended up being overdesigned.

Figure 5 shows a typical variation of the axial force magnification coefficient B_P with the number of floors and the number of bays, and Figure 6 shows a typical variation of the bending moment magnification coefficient B_M with the number of floors and the number of bays. The graphs shown correspond to the same first floor column in all the studied

	A	B	C	D	E	F	G	H	I	J	K	L	AD	AE	AF	AG
1	Member	No of Floors	No of Bays	Floor Height (ft)	Bay Length (ft)	Frame Spacing (ft)	Lb / Ly (ft)	Mem Type	SectNum	Size	Member Level	Member Position	B_1	B_2	R	Load Combination
2	1	2	2	15	15	20	5	Column	232	W12X16	1	1	1.0000	1.1454	0.827	15
3	2	2	2	15	15	20	5	Column	231	W12X19	1	2	1.0000	1.1454	0.882	14
4	3	2	2	15	15	20	5	Column	232	W12X16	1	3	1.0000	1.1454	0.827	14
5	4	2	2	15	15	20	5	Column	232	W12X16	2	1	1.0000	1.0152	0.347	3
6	5	2	2	15	15	20	5	Column	231	W12X19	2	2	1.0000	1.0152	0.186	11
7	6	2	2	15	15	20	5	Column	232	W12X16	2	3	1.0000	1.0152	0.347	2
8	7	2	2	15	15	20	0	Beam	231	W12X19	1	1	1.0025	1.0000	0.904	14
9	8	2	2	15	15	20	0	Beam	231	W12X19	1	2	1.0025	1.0000	0.904	15
10	9	2	2	15	15	20	5	Beam	233	W12X14	2	1	1.0038	1.0000	0.460	8
11	10	2	2	15	15	20	5	Beam	233	W12X14	2	2	1.0038	1.0000	0.460	9
12																

Fig. 2. Partial screen capture of results worksheet for a two-bay, two-floor system.

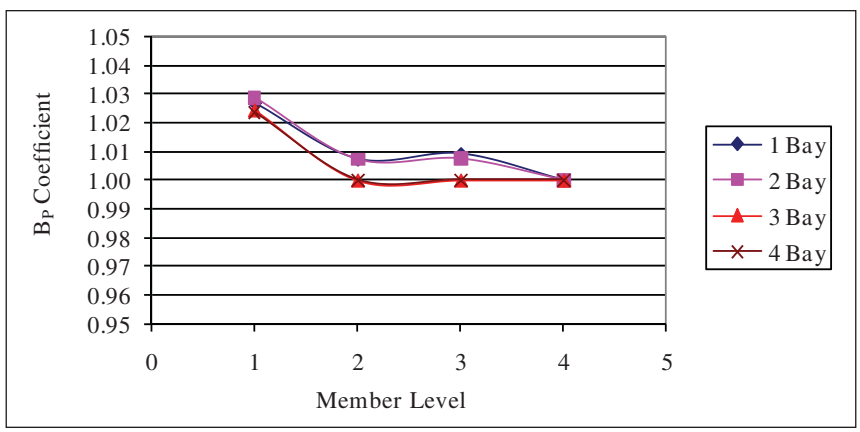

Fig. 3. Typical variation of the coefficient B_P *based on member level.*

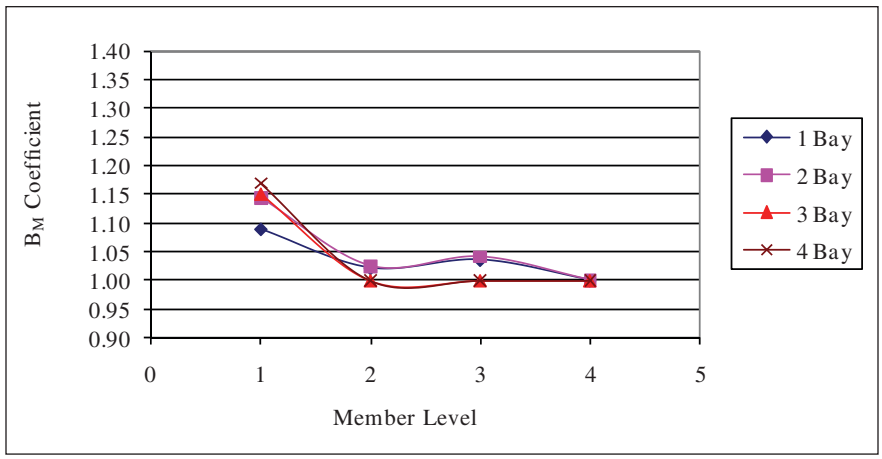

Fig. 4. Typical variation of the coefficient B_M *based on member level.*

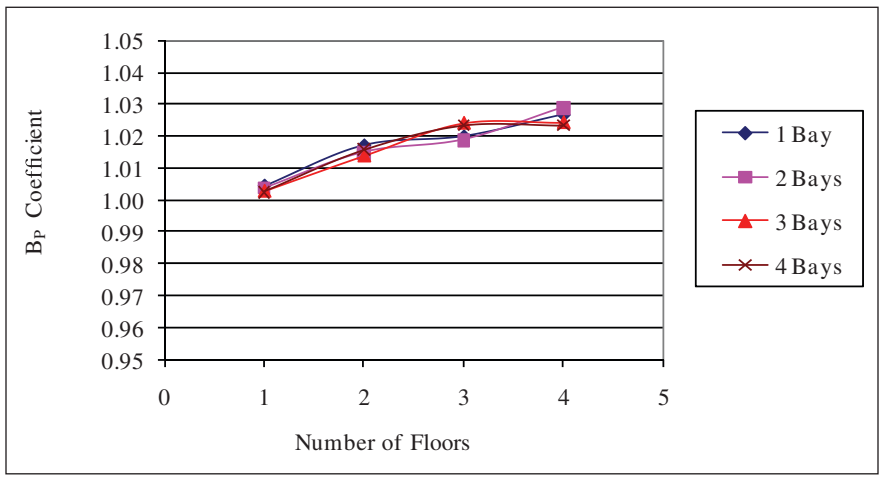

Fig. 5. Typical variation of the coefficient B_P *with the number of floors.*

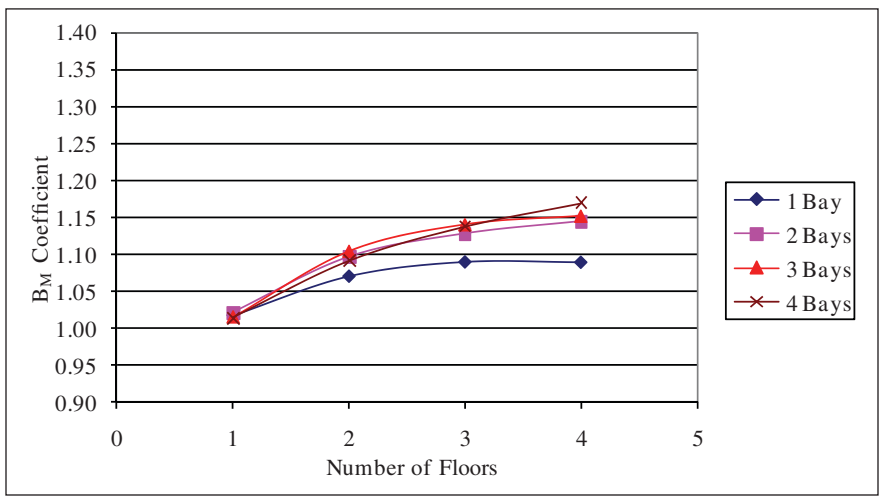

Fig. 6. Typical variation of the coefficient B_M *with the number of floors.*

systems and show a clear increase in the values of the magnification coefficients with an increase in the number of floors of the system. However, the number of bays seems to have a bigger effect on the moment magnification coefficient B_M than it has on the axial force magnification B_P, and this effect gets larger with a larger number of floors.

Because the objective of the study is to come up with a simplified axial force and bending moment magnification method, it was imperative to come up with a single variable to base these coefficients on; using member level, number of levels, and the number of bays in a structure will not produce a practical approach. The results from the aforementioned analyses indicate that there may be a correlation between the amount of axial load a column is subjected to and the axial force and bending moment amplification coefficients. To investigate this further, the variation of B_P and B_M with $(P_{nt} + P_{lt})/\phi P_n$ was examined. This ratio was selected because it incorporates not only applied loads but also geometric and material properties of the affected column. An initial study of the data revealed that a range of values of B_P and B_M can be associated with any single value of $(P_{nt}+P_{lt})/\phi P_n$. This is because the data represent a variety of columns that may be affected by *P*-delta effects to different degrees. The conservative approach was then to try to correlate maximum B_P and B_M values to $(P_{nt} + P_{lt})/\phi P_n$. To do this, the ratios of $(P_{nt} + P_{lt})/\phi P_n$ were divided into intervals of 0.05, and the maximum values of B_P and B_M were obtained for each interval and plotted. Figure 7 shows the variation of the maximum B_P coefficient with $(P_{nt} + P_{lt})/\phi P_n$ with a linear trend line ($R^2 = 0.9229$) and a quadratic trend line ($R^2 = 0.9468$). It is clear from this graph that a linear representation of the variation of B_P with $(P_{nt} + P_{lt})/\phi P_n$ is adequate and can be used as a basis for a simplified evaluation of this coefficient. Although the quadratic equation has a slightly higher R^2 value, the simpler format of the linear equation makes it a more practical choice.

Figure 8 shows the variation of the maximum B_M coefficient with $(P_{nt} + P_{lt})/\phi P_n$ with a linear trend line ($R^2 = 0.8689$) and a quadratic trend line ($R^2 = 0.8994$). Here again, the graph indicates that a linear representation of the variation of B_M with $(P_{nt} + P_{lt})/\phi P_n$ is adequate and can be used as a basis for a simplified evaluation of this coefficient.

PROPOSED DESIGN PROCEDURE

The following procedure is being proposed to account for second-order effects in the design of low-rise steel framed buildings. The methodology is based on using Equation C2-6a (AISC, 2005a), which does not depend on using drift as a parameter in calculating the amplification coefficient B_2. This procedure is applicable to pinned-base rigid-frame systems that have up to four floors, that are one to four bays wide and that have a beam length to frame height ratio between 1.5 and 2.2. Furthermore, all the limitations of the second-order analysis by amplified first-order analysis method that are stipulated in Appendix 8 of the 2010 AISC *Specification* apply to this proposed method as well. The method is presented as follows:

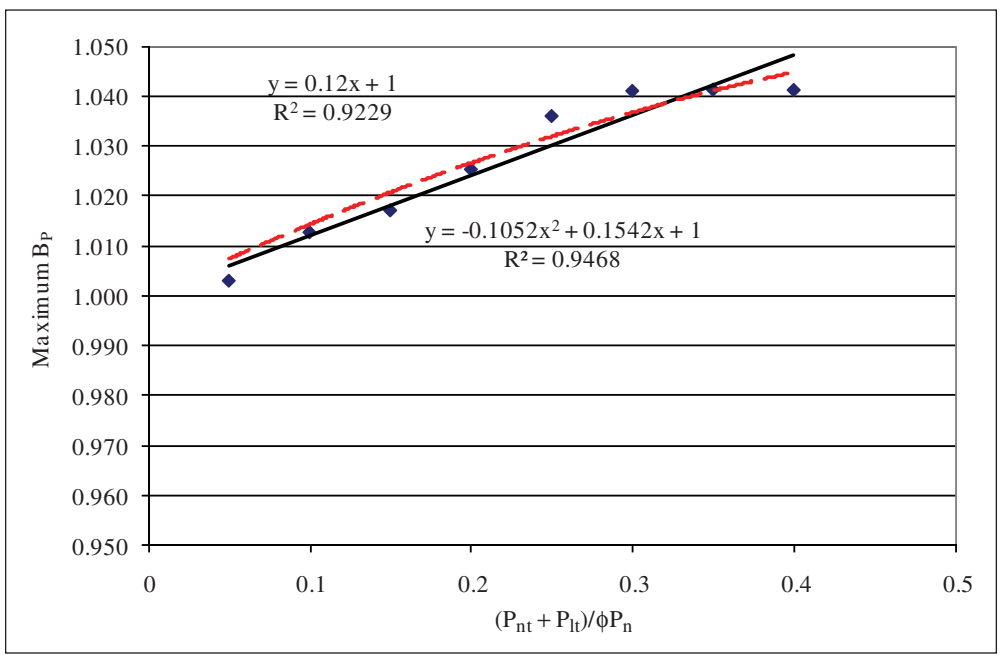

Fig. 7. Variation of maximum B_P *with* $(P_{nt} + P_{lt})/\phi P_n$.

- Analyze the structure for the simultaneous action of gravity and lateral loads, and obtain the total combined axial load (P_t) and the total combined bending moment (M_t) for the member under consideration using LRFD or ASD load combinations as appropriate.

- Compute the coefficient B_P:

$$\text{LRFD} \quad B_P = \frac{1}{8}\left(\frac{P_t}{P_{cx}}\right)+1$$

$$\text{ASD} \quad B_P = \left(\frac{2}{15}\right)\left(\frac{P_t}{P_{cx}}\right)+1$$

- Compute the coefficient B_M:

$$\text{LRFD} \quad B_M = \frac{1}{2}\left(\frac{P_t}{P_{cx}}\right)+1$$

$$\text{ASD} \quad B_M = \left(\frac{8}{15}\right)\left(\frac{P_t}{P_{cx}}\right)+1$$

- Compute the required axial strength:

$$\text{LRFD} \quad P_u = B_P P_t$$

$$\text{ASD} \quad P_a = B_P P_t$$

- Compute the required bending moment:

$$\text{LRFD} \quad M_u = B_M M_t$$

$$\text{ASD} \quad M_a = B_M M_t$$

where P_t is the total combined axial load, M_t is the total combined bending moment using LRFD or ASD load combinations as applicable, and P_c is ϕP_n for LRFD and P_n/Ω for ASD.

For structures that are up to two stories tall, and based on the discussion in the parametric analysis section of this paper, the following values may conservatively be used to amplify forces and moments obtained by a first order analysis:

- Use $B_P = 1.03$
- Use $B_M = 1.10$ for single-bay systems
- Use $B_M = 1.15$ for two-bay systems
- Use $B_M = 1.20$ for three-bay systems
- Use $B_M = 1.25$ for four-bay systems

The existence of gravity-only (leaning) columns can be accounted for by including their load in P_t (in the equations to compute B_P and B_M only) or by adjusting K_x. Several approaches are available in the AISC *Specification* Commentary (AISC, 2010) to include this effect, but the approach

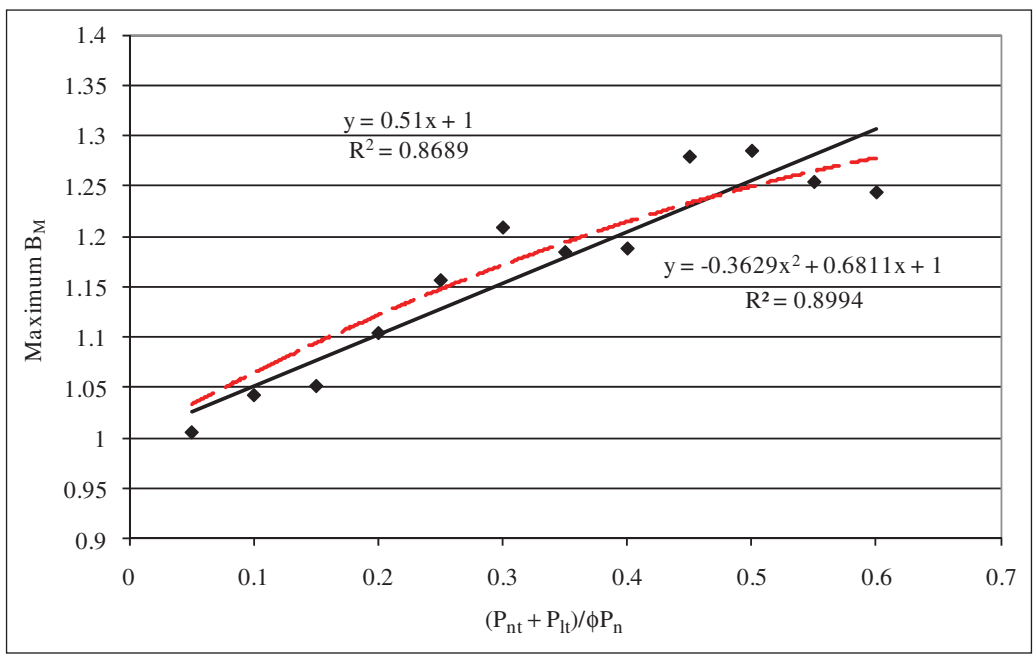

Fig. 8. Variation of maximum B_M *with* $(P_{nt} + P_{lt})/\phi P_n$.

Table 1. Comparison between Stability Analysis Methods (AISC, 2005) and Proposed Method for One-Bay Frame	
Method	**Interaction Equation**
Second-order	0.84
First-order	0.811
Direct analysis	0.796
Simplified	0.966
Proposed method	0.817

that was used by Carter and Geschwindner (2008) in their examples, which had been provided in previous commentaries (Lim and McNamara, 1972), is also used in this paper.

COMPARISON WITH EXISTING METHODS

Carter and Geschwindner (2008) used two simple frames to compare four methods of stability analysis and design:

1. Second-order analysis method (AISC 2005a, Section C2.2a)
2. First-order analysis method (AISC 2005a, Section C2.2b)
3. Direct analysis method (AISC 2005a, Appendix 7)
4. Simplified method (AISC 2005b, p. 2-12 and the AISC *Basic Design Values* cards).

A comparison between the proposed method presented in this paper and the results obtained by Carter and Geschwindner (2008) for a one-bay unbraced frame and a three-bay unbraced frame with leaning columns is presented.

One-Bay Frame

The trial shape (W14×90) used by Carter and Geschwindner for Column A in Figure 9 will be used for the comparison of the proposed method and the four methods of stability presented in the 2005 AISC *Steel Construction Manual*.

Based upon the loading shown in Figure 9, the first-order axial force, strong-axis moment and design parameters for Column A are:

$P_t = 200$ kips $\quad M_t = (20 \text{ kips})(15 \text{ ft}) = 300$ kip-ft
$L_x = L_y = 15$ ft $\quad K_x = 2.0 \quad K_y = 1.0$
$L_b = 15$ ft $\quad C_b = 1.67$

To be consistent with the comparison presented by Carter and Geschwindner (2008), the value of $K_x = 2.0$, the theoretical value for a column with a fixed base and a top that is free to rotate and translate, is used rather than the value of 2.1 recommended for design in the 2005 AISC *Specification* Commentary Table C-C2.2.

The effect of the leaning-column is calculated as

$$\Sigma P_{leaning} / \Sigma P_{stability} = (200 \text{ kips})/(200 \text{ kips}) = 1$$

$$K_x^* = K_x(1 + \Sigma P_{leaning}/\Sigma P_{stability})^{1/2} = 2.0(1+1)^{1/2} = 2.83$$

Based upon these design parameters, the axial and strong axis available flexural strengths of the ASTM A992 W14×90 are:

$P_c = \phi P_{nx} = 721$ kips $\quad M_{cx} = \phi_b M_{nx} = 573$ kip-ft

The new proposed amplification factors are:

$$B_p = \frac{1}{8}\left(\frac{P_t}{\phi P_{nx}}\right) + 1 = 1.035 \quad B_M = \frac{1}{2}\left(\frac{P_t}{\phi P_{nx}}\right) + 1 = 1.139$$

$$P_r = B_p P_t = (1.035)(200 \text{ kips}) = 207 \text{ kips}$$

$$M_{rx} = B_M M_t = (1.139)(300 \text{ kip-ft}) = 341.7 \text{ kip-ft}$$

$P_r/P_c = 207/721 = 0.287$. Because $P_r/P_c \geq 0.2$, Equation H1-1a is applicable.

$$\frac{P_r}{P_c} + \frac{8}{9}\left(\frac{M_{rx}}{M_{cx}}\right) = 0.287 + \frac{8}{9}\left(\frac{341.7}{573}\right) = 0.817$$

Table 1 shows that the proposed method of predicting the required strength of the stability column in the one-bay frame shown in Figure 9 is comparable to the other stability methods studied by Carter and Geschwindner (2008).

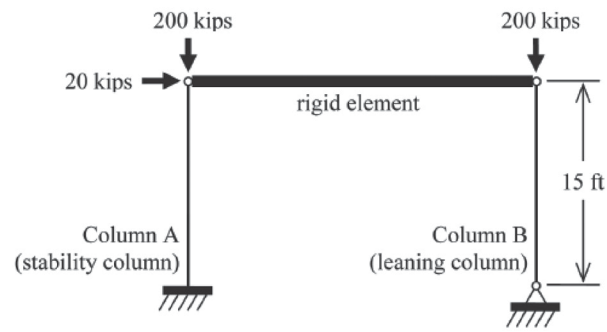

Fig. 9. One-bay unbraced frame used in examples by Carter and Geschwindner (2008).

Table 2. Comparison between Stability Analysis Methods (AISC, 2005) and Proposed Method for Three-Bay Frame	
Method	**Interaction Equation**
Second-order	0.232
First-order	0.239
Direct analysis	0.235
Simplified	0.240
Proposed method	0.245

Three-Bay Frame

The trial shape (W14×109) used by Carter and Geschwindner for Column D will be used for the comparison of the proposed method and the four methods of stability presented in the 2005 AISC *Steel Construction Manual*.

Based upon the loading shown in Figure 10, the first-order axial force, strong-axis moment and design parameters for Column A are:

$P_t = 150$ kips $\quad M_t = (15 \text{ kips})(15 \text{ ft})/2 = 113$ kip-ft

$L_x = L_y = 15$ ft $\quad K_x = 2.0 \quad K_y = 1.0$

$L_b = 15$ ft $\quad C_b = 1.67$

The effect of leaning-column is calculated as:

$$\Sigma P_{leaning} / \Sigma P_{stability} = 2(75 \text{ kips})/[2(150 \text{ kips})] = ½$$

$$K_x^* = K_x(1 + \Sigma P_{leaning} / \Sigma P_{stability})^{½}$$
$$= 2.0\ (1 + 0.5)^{½}$$
$$= 2.45$$

The *y*-axis effective length is calculated as:

$$K_y L_y = 15 \text{ ft}$$

The equivalent *x*-axis effective length is calculated as:

$$\frac{k_x^* L_x}{r_x / r_y} = \frac{(2.45)(15)}{1.67} = 22 \text{ ft (governs)}$$

Based upon these design parameters, the axial and strong axis available flexural strengths of the ASTM A992 W14×109 are:

$$P_c = \phi P_n = 1000 \text{ kips}$$

$$M_{cx} = \phi_b M_{nx} = 720 \text{ kip-ft}$$

The new proposed amplification coefficients are:

$$B_p = \frac{1}{8}\left(\frac{P_t}{\phi P_{nx}}\right) + 1 = 1.01 \quad B_M = \frac{1}{2}\left(\frac{P_t}{\phi P_{nx}}\right) + 1 = 1.075$$

$$P_r = B_p P_t = (1.019)(150 \text{ kips}) = 152.85 \text{ kips}$$

$$M_{rx} = B_M M_t = (1.075)(113 \text{ kip-ft}) = 121.48 \text{ kip-ft}$$

$P_r / P_c = 152.85/1000 = 0.153$. Because $P_r/P_c < 0.2$, Equation H1-1b is applicable.

$$\frac{P_r}{2P_c} + \left(\frac{M_{rx}}{M_{cx}}\right) = \frac{0.153}{2} + \left(\frac{121.48}{720}\right) = 0.245$$

Table 2 shows that the proposed method prediction of the interaction equation is approximately the same as that predicted by the other stability method studied by Carter and Geschwindner (2008), and there is no significant change among all the methods studied for the three-bay frame.

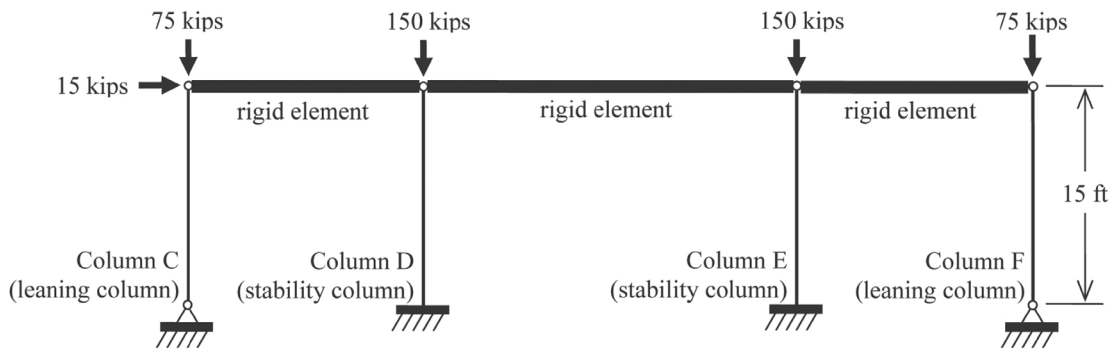

Fig. 10. Three-bay unbraced frame used in examples Carter and Geschwindner (2008).

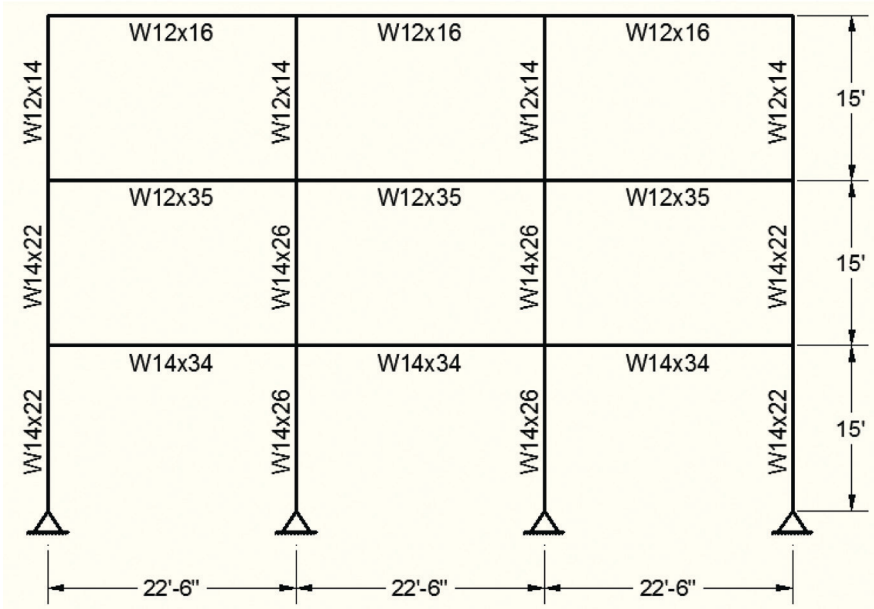

Fig. 11. Three-bay, three-floor system design example.

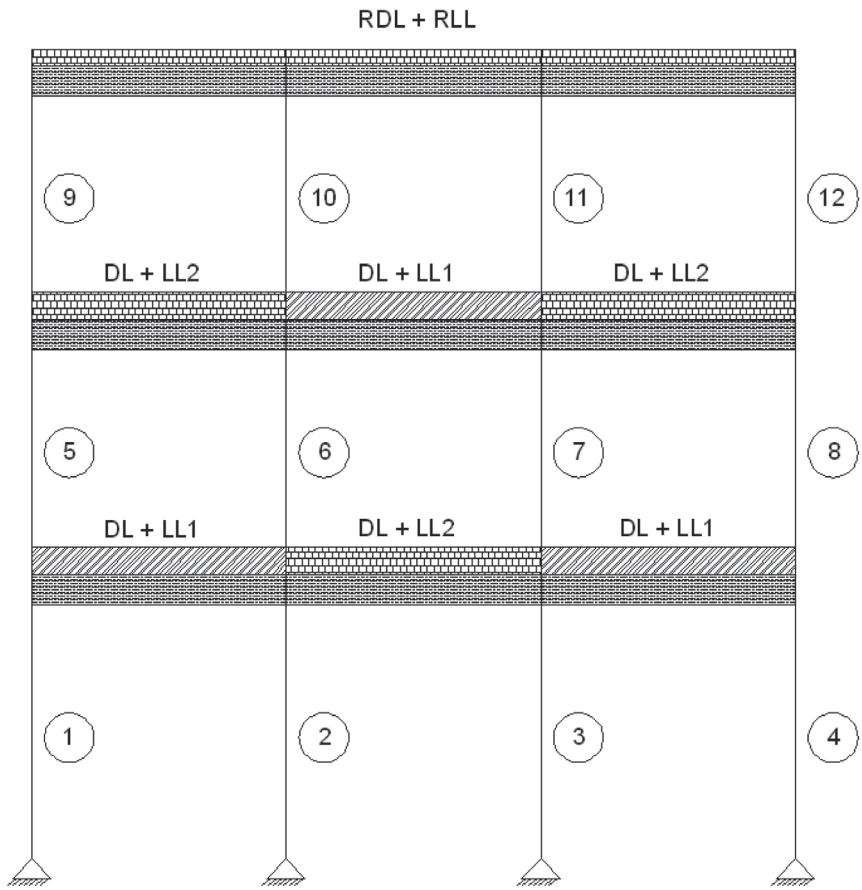

Fig. 12. Three-bay, three-floor system under gravity loading.

DESIGN EXAMPLE

The three-bay, three-floor frame system shown in Figure 11 was used to illustrate the use of the proposed method. The frame is subjected to a floor dead load of 80 psf, a floor live load of 50 psf, and roof dead and live loads of 25 psf and 20 psf, respectively. Frames were assumed to be spaced at 20 ft, and two alternate live loading cases were created to obtain the maximum possible efforts in each member. The total seismic base shear was 12.2 kips, and the total wind force was 10 kips. No consideration was taken for practicality or member connectivity to ensure that strength requirements control the design.

The frame is designed twice: once using the 2005 AISC *Specification* amplified first-order elastic analysis method, and second using the proposed design procedure. The results of the analyses are then compared. First the system is analyzed under gravity loads (as shown in Figure 12), and the first-order axial force (P_{nt}) and the first-order moment (M_{nt}) are computed for each frame member, assuming there is no lateral translation of the frame. The frame is then analyzed for lateral loads (as shown in Figure 13), and the first-order axial force (P_{lt}) and the first-order moment (M_{lt}) caused by lateral translation of the frame are computed for each frame member. The moment amplification coefficients B_1 and B_2 are then computed, and the required axial and flexural strengths of all frame members are evaluated.

According to the proposed design procedure, the frame is only analyzed once under the simultaneous action of gravity and lateral loads (as shown in Figure 14), and the total factored axial load (P_t) and total factored moment (M_t) are computed for each frame member. The coefficients B_P and B_M are then computed using the proposed equations. The required axial and flexural strengths of each member are then computed by multiplying the total factored axial load by the coefficient B_P and the total factored bending moment by the coefficient B_M, respectively. The results of the design of this three-bay, three-floor system are shown in Table 3.

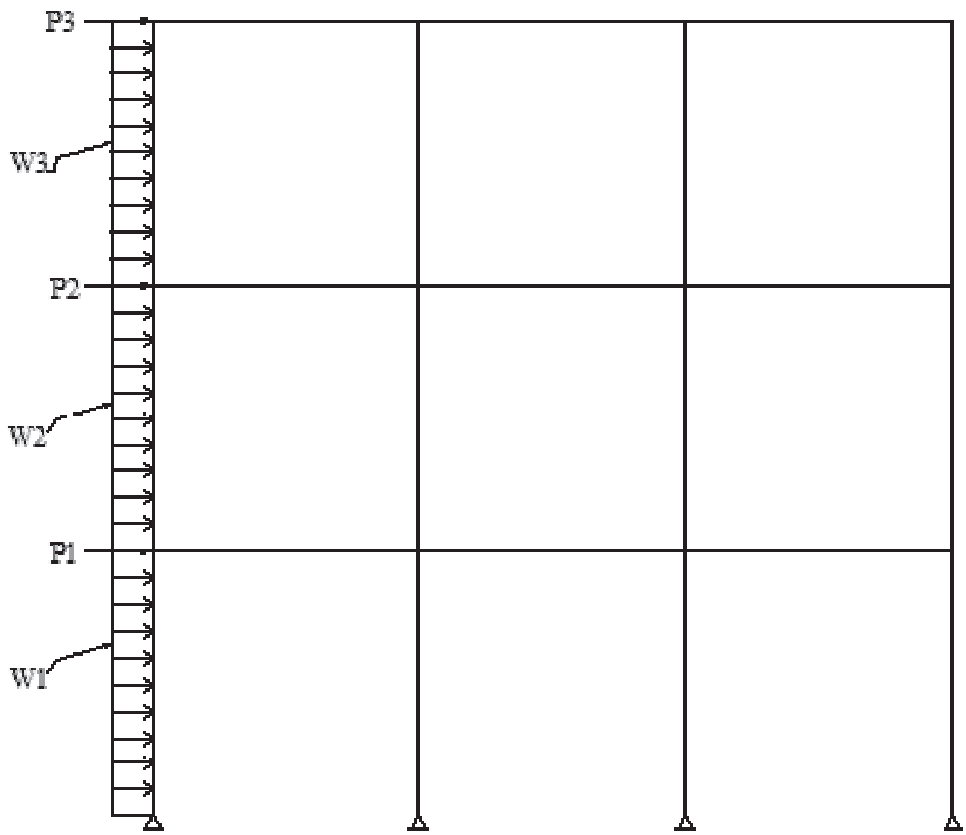

Fig. 13. Three-bay, three-floor system under lateral loading.

Table 3. Design Results of Three-Bay, Three-Floor Frame							
Column	Based on B_1 and B_2			Based on B_P and B_M			% increase in R
	P_u, kip	M_u, kip-ft	R	P_u, kip	M_u, kip-ft	R	
1	66.77	−69.95	0.833	67.84	−71.34	0.885	6.24
2	131.56	68.78	0.923	139.95	70.78	0.944	2.27
3	131.56	−68.78	0.923	139.95	−70.78	0.944	2.27
4	66.71	69.91	0.832	67.80	71.30	0.884	6.24
5	45.57	−74.75	0.746	46.78	−82.69	0.912	22.23
6	65.99	44.20	0.510	68.03	48.02	0.544	6.77
7	65.96	−44.14	0.509	67.99	−47.96	0.544	6.78
8	45.57	74.75	0.746	46.78	82.69	0.912	22.23
9	12.97	−35.11	0.595	13.15	−37.05	0.739	24.18
10	14.41	−20.11	0.372	14.64	−21.04	0.414	11.22
11	14.40	19.97	0.370	14.62	20.89	0.411	11.13
12	12.97	35.11	0.595	13.15	37.05	0.739	24.18

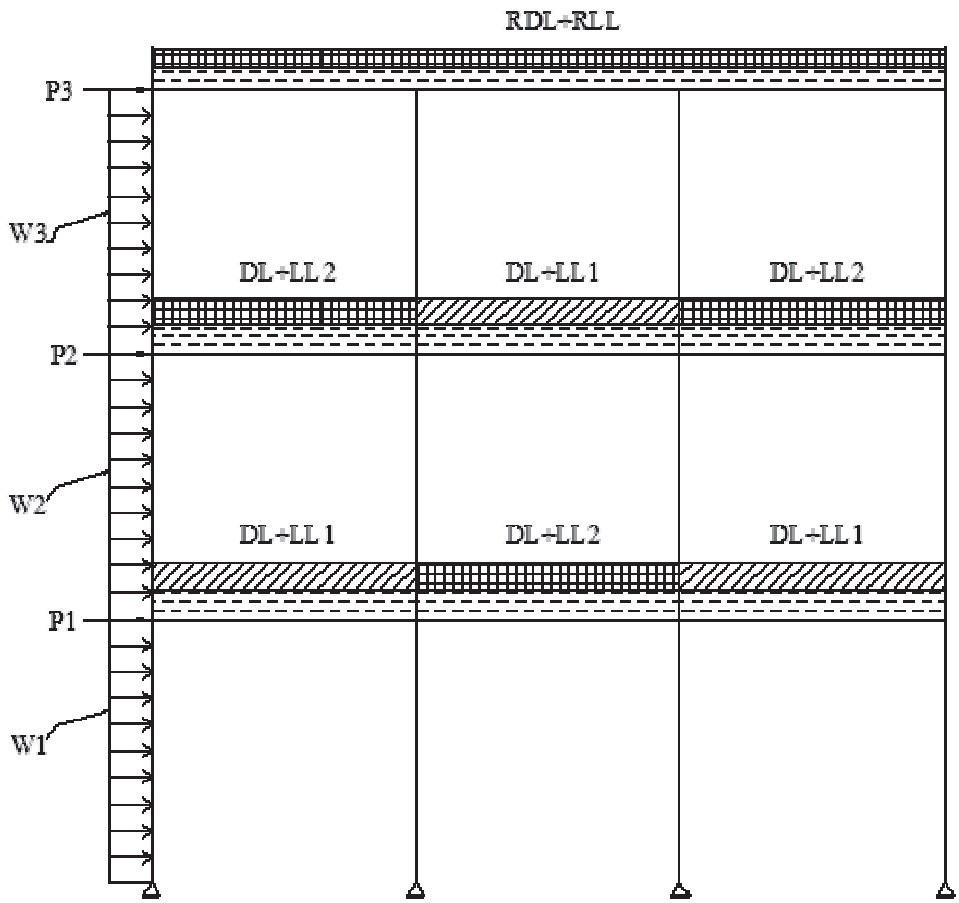

Fig. 14. Three-bay, three-floor system under combined loading.

CONCLUSIONS

A simplified procedure for the evaluation of second-order effects by amplified first-order analysis is proposed in this paper. The procedure applies to the design of low-rise steel-framed buildings. This procedure was compared to four other established design procedures and was found to produce similar results. Moreover, a typical three-bay, three-floor frame was designed using the 2010 AISC approximate second-order analysis, and the proposed method and the results were compared. It is interesting to see in this example that the columns that show the largest increase in the values of the design ratio are in the upper two floors of the structure. It was shown earlier in this study that the design of these columns is usually not affected by the inclusion of second-order effects. They typically carry a light load, causing the member size selection to be controlled by practical rather than strength considerations. They typically carry a light load; consequently, a small increase in that load will translate in a more significant increase in terms of percentage.

The procedure being proposed herein has the advantage of being very straightforward and simple to apply because it only requires a single elastic analysis using existing real loads. Amplified design forces are then obtained by multiplying the first-order analysis results by simple magnification coefficients that are based on the ratio of the applied load to the computed column design strength.

ACKNOWLEDGMENT

The study reported herein was conducted by Maulik Patel in fulfillment of the requirements for a master's of science degree in civil engineering under the direction of Dr. Souhail Elhouar, P.E., associate professor of civil engineering and construction. The support of the Bradley University Department of Civil Engineering and Construction toward the completion of the research that led to this publication is hereby acknowledged.

REFERENCES

AISC (1989), *Specification for Structural Steel Buildings, Allowable Stress Design and Plastic Design*, American Institute of Steel Construction, Chicago, IL.

AISC (1993), *Load and Resistance Factor Design Specification for Structural Steel Buildings*, American Institute of Steel Construction, Chicago, IL.

AISC (1999), *Load and Resistance Factor Design Specification for Structural Steel Buildings*, American Institute of Steel Construction, Chicago, IL.

AISC (2005a), *Specification for Structural Steel Buildings*, ANSI/AISC 360-05, American Institute of Steel Construction, Chicago, IL.

AISC (2005b), *Steel Construction Manual,* 13th ed., American Institute of Steel Construction, Chicago, IL.

AISC (2010), *Specification for Structural Steel Buildings*, ANSI/AISC 360-10, American Institute of Steel Construction, Chicago, IL.

Becker, D. (2008), "Consideration of the Effects of Loading and Frame Configuration Using the Direct Analysis Method," Crossing Borders, *Proceedings, 2008 Structures Congress,* April 24–26, Vancouver, BC, Canada.

Carter, C.J. and Geschwindner, L.F. (2008), "A Comparison of Frame Stability Analysis Methods in ANSI/AISC 360-05," *Engineering Journal*, AISC, Third Quarter, pp. 159–170.

Carter, C.J., Murray, T.M. and Thornton, W.A. (2000), "Cost Effective Steel Building Design—The U.S. Approach," *Progress in Structural Engineering and Materials*, Vol. 2, No. 1, John Wiley and Sons, Ltd., U.K., January–March, pp. 16–25.

Chen, S.J. and Wang, W.C. (1999), "Moment Amplification Factor for P-Δ Effect of Steel Beam-Column," *Journal of Structural Engineering*, ASCE, Vol. 125, No. 2, July, pp. 219–233.

Duan, L. and Chen, W.-F. (1989), "Design Interaction Equation for Steel Beam-Columns," *Journal of Structural Engineering*, ASCE, Vol. 115, No. 5, May, pp. 1225–1243.

Eroz, M., White, D. and DesRoches, R. (2008), "Direct Analysis and Design of Steel Frames Accounting for Partially Restrained Column Base Condition," *Journal of Structural Engineering*, ASCE, Vol. 134, No. 9, pp. 1508–1517.

Kim, S.-E. and Choi, S.-H. (2005), "Practical Second-Order Inelastic Analysis for Three-Dimensional Steel Frames Subjected to Distributed Load," *Thin Walled Structures*, Elsevier, Vol. 43, No. 1, January, pp. 135–160.

Lim, L.C. and McNamara, R.J. (1972), "Stability of Novel Building System," Structural Design of Tall Buildings, Vol. II-16, *Proceedings*, ASCE-IABSE International Conference on the Planning and Design of Tall Buildings, Bethlehem, PA, pp. 499–524.

Sohal, I.S. and Syed, N.A. (1992), "Inelastic Amplification Factor for Design of Steel Beam-Columns," *Journal of Structural Engineering*, ASCE, Vol. 118, No. 7, July, pp. 1822–1840.

Surovek, A. and Ziemian, R. (2005), "The Direct Analysis Method: Bridging the Gap from linear Elastic Analysis to Advanced Analysis in Steel Frame Design," *Proceedings, 2005 Structures Congress and the 2005 Forensic Engineering Symposium*.

The Effect of Piece Marking on Fatigue Performance of Bridge Steel

KARL H. FRANK, VASILIS SAMARAS and TODD A. HELWIG

ABSTRACT

An experimental study was undertaken to determine if markings used to identify fabricated steel using modern automatic impact stenciling equipment could be used on structures subjected to fatigue loading. The fatigue specimens with both numeric and alphabetic markings were tested. The results showed that the fatigue life of marked steel exceeded the fatigue design strength for Category A, the highest fatigue design category. Marking pieces with this equipment will not affect the fatigue design strength of the member.

Keywords: marking, fatigue, stamps, bridges.

INTRODUCTION

Steel components are marked during fabrication to help track the pieces through the fabrication process and ultimately to provide the erector with a method of identifying the correct location of the piece in the structure. Splice plates and the mating members are marked to ensure the correct orientation and location of the matched drilled pieces. A matched mark web member in a truss and gusset plate is shown Figure 1.

Typically, the marking has been performed manually using die stamps. The die stamps specified are often called out as low-stress stamps. The low stress refers to low increase in stress caused by the stamp. Die stamps labeled as low stress are available in the marketplace, but it is often not clear which specification these stamps satisfy. MIL-STD-792F(SH), *The Department of Defense Manufacturing Process Standard Identification Marking Requirements for Special Purpose* (Department of Defense, 2006), spells out the some of geometric requirements for low-stress stamps, shown in Table 1. The indentation is specified to be a round bottom with the minimum radius given in the table as opposed to the sharp "V" found on normal stamps. The specification also limits the depth of the stamp to a shallow 0.010 in.

Other marking techniques are available: the stamping can be done with a powder-actuated gun, inkjet stenciling, scribing, plasma torch, or impact stylus system. It is desirable to have a marking system that can be integrated into the numerical controlled cutting equipment currently in use in the steel fabricating industry. The pieces can be marked as they are cut, eliminating the possibility of mismarking pieces that look identical but may have slight differences in geometry. The marking should ideally be visible after application of paint and provide a permanent mark. In addition, the marking should not reduce the tensile and fatigue strength of the component.

A research study was conducted to determine the effect of marking using a computer-controlled impact stylus system. The system has been used in a semi-automatic mode to mark components for building and other nonbridge structures. It is a fast and flexible system that can be mounted and interfaced with existing equipment used for cutting the plates. The object of the research was to determine if steel marked with this system would have a reduced fatigue life or tensile strength.

The equipment used to perform the marking is manufactured by Couth of Spain. An electromechanical model MC2000 was used to mark the specimens. A picture of the equipment is shown in Figure 2. A typical mark made by the equipment is shown in Figure 3. The Gulim font used was used with a character height of 14 mm (0.55 in.). The stylus force was 150 lb. Note the larger and deeper indentations at the intersections formed at start and stop of the segments of the character.

SPECIMEN DESIGN, FABRICATION AND TESTING PROCEDURE

The fatigue specimens were designed to be tested in a closed-loop, 22-kip capacity, axial load testing frame. The test frame has hydraulically actuated grips that limited the thickness of the specimens. The width of the specimen was selected to provide a wide enough surface to accommodate

Karl H. Frank, Chief Engineer, Hirschfeld Industries, Austin, TX (corresponding author). E-mail: karl.frank@hirschfeld.com

Vasilis Samaras, Graduate Research Assistant, University of Texas at Austin, Austin, TX. E-mail: vasamara@gmail.com

Todd A. Helwig, Associate Professor, University of Texas at Austin, Austin, TX. E-mail: thelwig@mail.utexas.edu

Table 1. Low-Stress Stamp Geometric Requirements		
Character Size (in.)	**Minimum Tip Radius (in.)**	**Nominal Impression Width for 0.010-in. Depth (in.)**
1/16	0.005	0.020
3/32	0.006	0.021
1/8	0.007	0.022
3/16	0.008	0.026
1/4	0.010	0.031
3/8	0.014	0.042
1/2	0.020	0.062

the 7/16-in.-tall markings. The coupon-shaped specimen shown in Figure 4 was fabricated from ½-in. A709 Grade 50 plate. Two sets of specimens were made, one set with alphabetic and another with numeric marking. Two orientations of the characters were marked on each specimen. The marking was oriented 90 degrees from the opposite side to test both possible character orientations in one specimen. The specimens were flame cut and the edges ground smooth; the mill scale was left intact. The impact stylus used to mark the specimen is shown in Figure 5.

The chemistry and mechanical properties of the plate reported by the mill are given in Table 2.

The specimens were tested in the 22-kip closed axial test frame shown in Figure 6. The loading was tension to tension at a constant stress range of either 30 or 35 ksi. The minimum stress was 5 ksi for all specimens. The cyclic loading frequency was approximately 10 Hz. The tests were run continuously until either the specimen fractured or the test was deemed a runout.

After the fatigue tests were completed, two of the fatigue

Fig. 1. Example of stamped piece marking at a connection.

Table 2. Mill Test Results of Test Plate Material										
Element	C	Mn	P	S	Si	Cu	Ni	Cr	V	Nb
Percent	0.18	0.99	0.011	0.002	0.17	0.27	0.08	0.09	0.030	0.002
Yield Strength			59.8, 64.6 ksi			**Tensile Strength**			82.3, 80.6 ksi	

Table 3. Fatigue Test Results					
Specimen Type	**Stress Range (ksi)**	**Specimen**	**Number of Fatigue Cycles**	**Test Outcome**	**Ratio Test Cycles to Category A Design Life**
Alphabetic	30	A1	2,700,241	Runout	1.7
	35	A2	2,672,452	Failed	4.6
		A3	6,000,028	Runout	10.3
		A4	7,513,600	Runout	12.9
		A5	9,241,204	Runout	15.8
Numeric	30	N1	2,674,040	Runout	1.7
	35	N2	3,181,753	Runout	5.5
		N3	6,009,136	Runout	10.3
		N4	5,079,358	Failed	8.7
		N5	6,826,604	Runout	11.7

specimens—one alphabetic and one numeric—that had not failed were loaded to failure in a larger test machine. As a control, an unmarked untested specimen without marking was also tensile tested.

FATIGUE TEST RESULTS

The initial two test specimens, one of each type of character, were tested at a stress range of 30 ksi. The testing was stopped after 2.7 million cycles. No cracking was found on the specimens. It was decided to test the next specimens at a 35-ksi stress range. The maximum stress of 40 ksi at 35-ksi stress range required almost 22 kips of force, the capacity of the test frame. The remaining specimens were tested at 35-ksi stress range. During the design of the specimens, it was assumed that they would fail before 1 million cycles, comparable to Category B of the fatigue specifications in AASHTO LRFD Bridge Specifications (2010). Only two specimens failed at the higher stress of 35 ksi. A summary of the test results is shown in Table 3.

Only two of the specimens failed, one of each type. The location of fatigue fractures are shown in Figures 7 and 8. The failures did not initiate at the deeper indentations that

Fig. 2. Marking tool and controller.

Fig. 3. Piece marking made with impact stylus system.

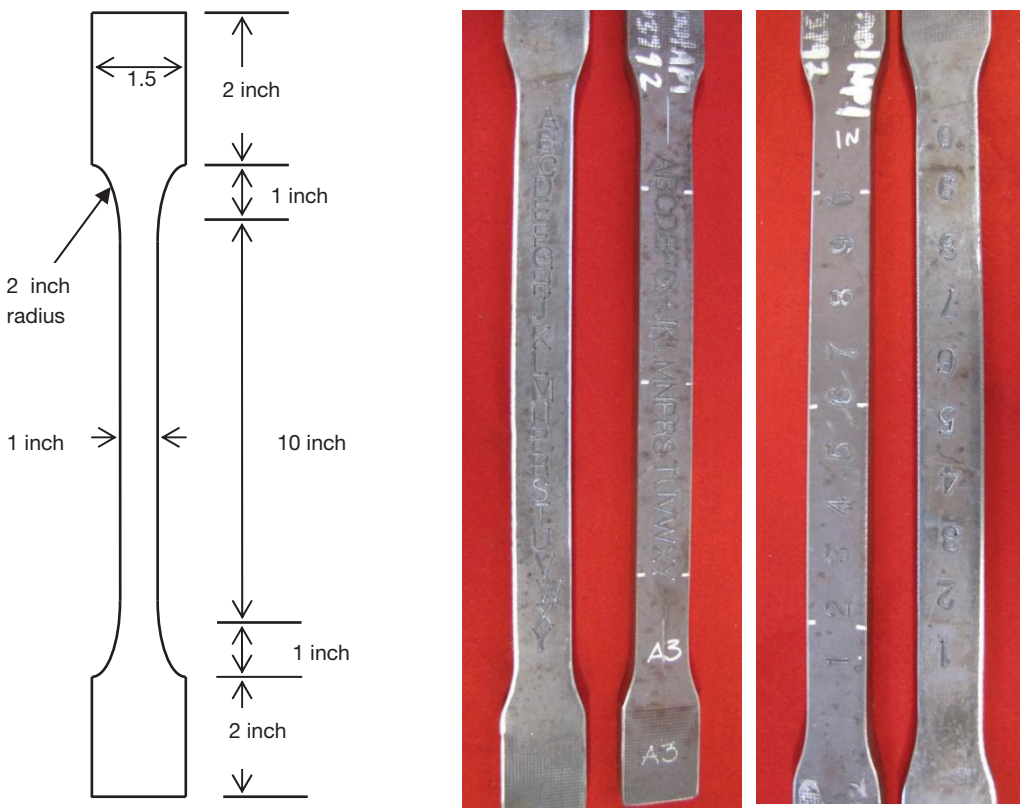

Fig. 4. Specimen configuration and marking.

occur at the intersections of character segments. The alphabetic specimen failure initiated at the letter "B" and the numeric at the numeral "1."

TENSION TEST RESULTS

The results of the tension tests done on the longest life fatigue specimens and an unmarked specimen are plotted in Figure 9. The plot shows the applied stress versus the cross head displacement. The yield and tensile strength of the marked specimen and fatigue tested specimens were similar to the unmarked control specimen.

DEPTH OF MARKINGS

The depths of the markings were measured using a thread micrometer. The pointed tip of the micrometer fit inside the indentation of the marking stylus. A minimum of three locations were measured on each character. The intersections of the character elements were included in the measurements because these appeared to have the greatest depth. A histogram of the measurements is shown in Figure 10. Two distinct peaks are evident; the first peak, at 0.010 in., is the depth away from the intersection. The second peak, at 0.017 in., is from the measurements at the intersections of character segments. The mean depth of all locations was 0.011 in. The maximum depth was 0.023 and the minimum was 0.004 in.

CONCLUSIONS

The marking of the specimens with electronically controlled impact stylus did not lower the fatigue strength specimens below the design strength for base metal in the AASHTO fatigue specifications. The design fatigue life of the marked material can be classified as Category A, the highest fatigue category. The markings, although slightly deeper than the military specification requirements, can safely be used on steel structures without concern for its effect on design fatigue performance. The tensile strength of the marked specimens was not reduced after subjecting the specimens to a 35-ksi stress range for more than 6 million cycles of loading.

REFERENCES

Department of Defense (2006), *Department of Defense Manufacturing Process Standard Identification Marking Requirements for Special Purpose Components*, MIL-STD-792F(SH), Washington, DC.

AASHTO (2010), *AASHTO LRFD Bridge Design Specifications*, 5th edition, AASHTO, Washington, DC.

Fig. 5. Stylus used to mark specimen.

Fig. 6. Specimen in test frame.

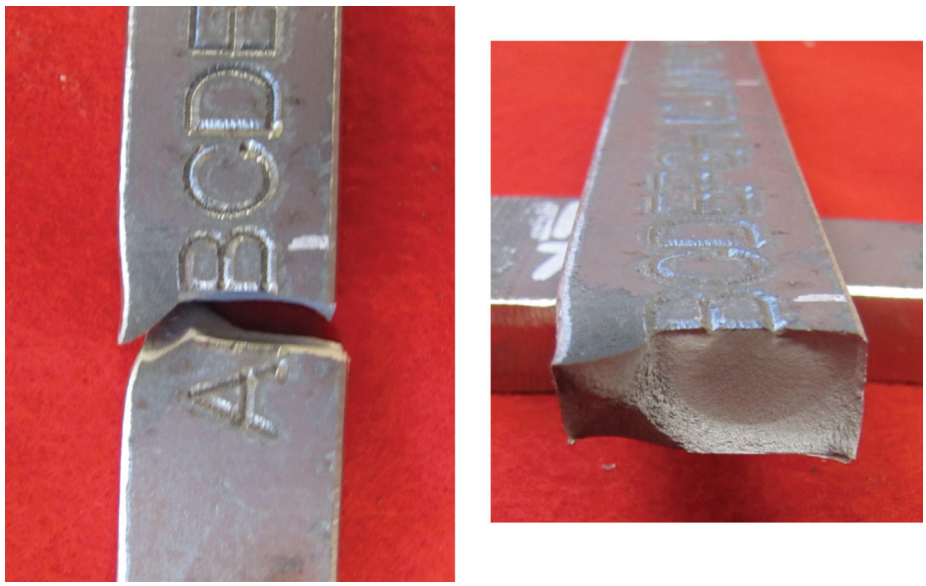

Fig. 7. Fatigue failure of alphabetic specimen.

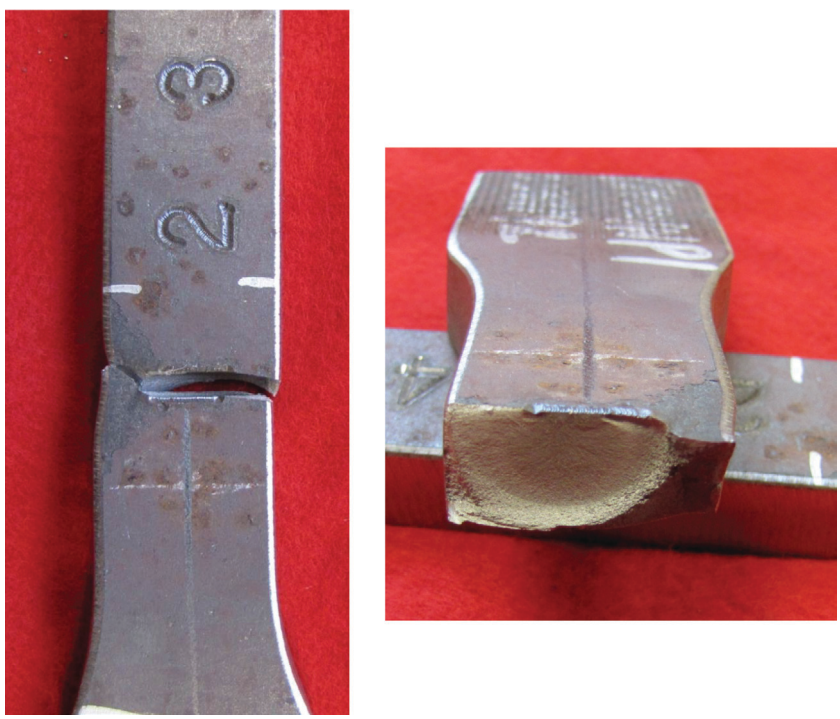

Fig. 8. Fatigue failure of numeric specimen.

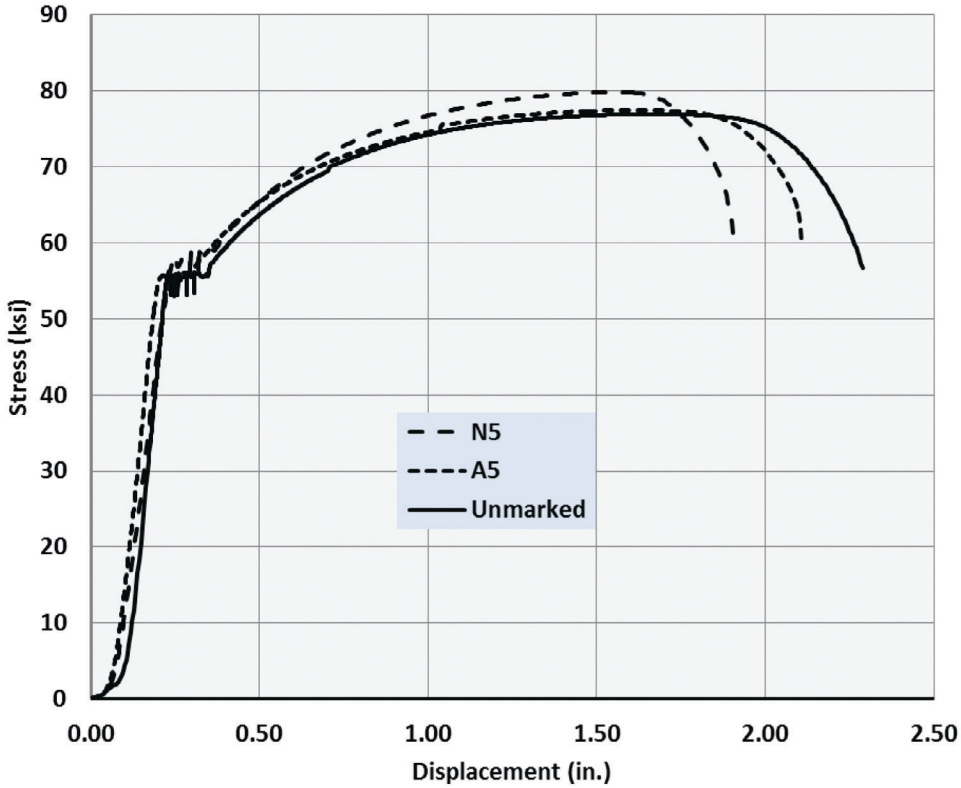

Fig. 9. Tensile test results.

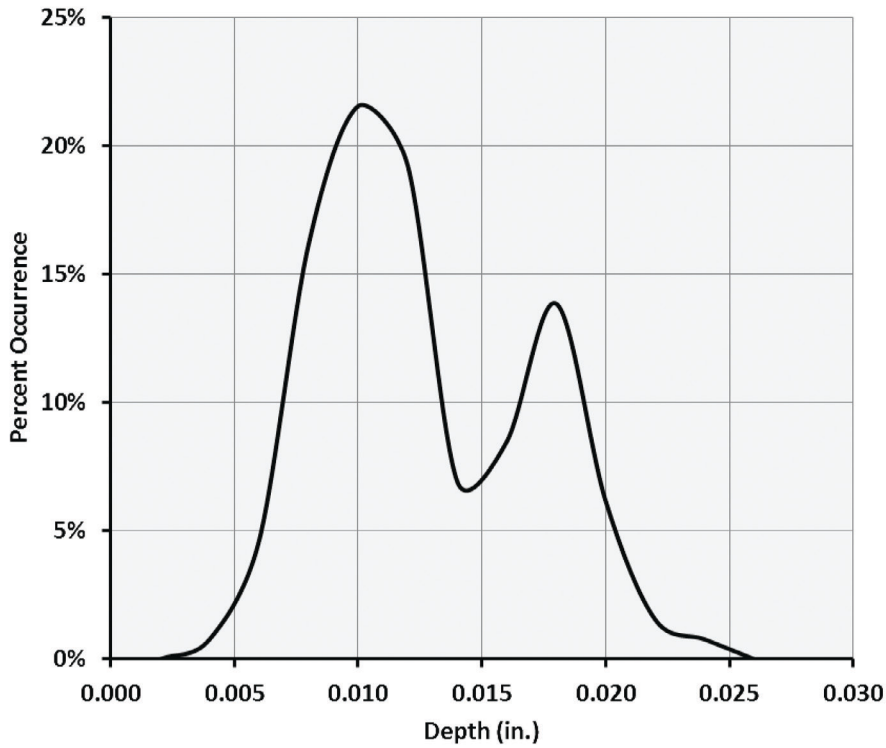

Fig. 10. Depth of stylus indentation.

Current Steel Structures Research
No. 30

REIDAR BJORHOVDE

INTRODUCTION

This issue of "Current Steel Structures Research" for the *Engineering Journal* focuses on a selection of research projects at universities in Europe and South America. The descriptions will not discuss all of the current projects at the schools. Instead, selected studies provide a representative picture of the research work and demonstrate the importance of the schools to the home countries and, indeed, to the efforts of industry and the profession worldwide.

The universities and many of their researchers are very well known in the world of steel construction: the "Rheinisch-Westphälische Technische Hochschule Aachen" (now commonly referred to as RWTH Aachen), located in the city of Aachen, Germany; the Federal University of Rio de Janeiro in Brazil; and the University of Chile in Santiago, Chile. The studies that are presented reflect elements of the projects as well as other major, long-time activities. All of the projects are multi-year efforts, emphasizing the need for careful planning and implementation of research needs and applications, including the education of graduate students and advanced researchers. As is also always the case in the United States, the outcomes of the studies focus on design standards and industry needs.

The lead researchers have been active for many years, as evidenced by their leading roles in the design standards development of their countries, but they have also been frequent participants in the work of other countries and regions. Large numbers of English-language technical papers and conference presentations have been published, contributing to a collection of studies that continue to offer solutions to complex problems for designers as well as fabricators and erectors. Many of the projects also complement current work in the United States and elsewhere. The broad sharing of knowledge that is taking place promises significant results, not the least because of issues of finances and the sheer cost of research: synergism is a critical feature of multi-institutional, indeed multinational activities.

References are provided throughout the paper, whenever such are available in the public domain. However, much of the work is still in progress, and in some cases, reports or publications have not yet been prepared for public dissemination.

Reidar Bjorhovde, Dr.-Ing., Ph.D., P.E., Research Editor of the *Engineering Journal.* Tucson, AZ. E-mail: rbj@bjorhovde.com

SOME CURRENT RESEARCH WORK AT RWTH AACHEN IN AACHEN, GERMANY

Established in 1870, RWTH Aachen has been one of the leading engineering academic institutions in Germany and Europe for many years. Steel structures research is performed under the auspices of the Institute of Steel Construction (ISC). For many years, the projects focused exclusively on steel and composite buildings and bridges, but in the 1980s, building aerodynamics and lightweight metal structures were added. In the 1990s, a number of projects with glass and steel and composite materials were also undertaken. Recognizing the importance of standards for all areas of construction, the institute has been heavily involved in the European design code development for more than 30 years. Most projects, therefore, aim at providing design criteria for structures and structural elements.

Under the leadership of Professor Markus Feldmann and, previously, Professor Emeritus Gerhard Sedlacek, the total annual research expenditures of the institute have typically amounted to €2.8 million (approximately $3.7 million in current funds). More than two-thirds of these funds are provided by external agencies—such as various ministries and commissions of the European Union—as well as by industry. RWTH Aachen is also a partner in many of the multi-university, multinational research projects that are under way in Europe at any one time; these efforts are strongly supported by the European Union, as well as the individual countries.

The current projects of the institute address major topics of steel and composite structures:

- All aspects of the stability of members and frames, as well as plate buckling.
- Performance considerations for steel, including brittle fracture and fatigue, as well as the unique demands of welded construction.
- Bridge engineering in general, including integrated abutments and bridge dynamics.
- Strength and behavior of new composite shear connections.

- Strength, ductility and stiffness of new types of connections using adhesive bonding.
- Wind towers for energy production, including new connection types and foundations.
- All aspects of sustainability.
- Static and dynamic response of buildings and bridges under wind loads.
- Glass engineering, including structural uses of glass, the strength and stability of columns, shear panels and beams of toughened and laminated panels or steel-glass composites.

Flexural and Lateral-Torsional Buckling of Steel Frames by a General Second-Order Approach: Professor Markus Feldmann is the project director, and the primary researchers from Aachen are Matthias Wieschollek, Nicole Schillo and Johannes Naumes. The project is sponsored by the German council of steel construction, along with the Federal Ministry of Economics.

Hot-rolled wide-flange shapes and similar welded sections have high in-plane strength about the strong axis. For efficient member performance, this should be exploited by preventing lateral-torsional buckling. The current rules of Eurocode 3 (ECS, 2005) provide for out-of-plane stability checks that can be performed according to one of the following methods: (1) a method using second-order analysis for which equivalent geometric imperfections are defined and (2) a method with member checks using flexural or lateral torsional buckling curves.

The research work treats out-of-plane stability checks using second-order analysis with equivalent geometric imperfections that have been defined in Eurocode 3 in agreement with elastic buckling modes. The use of out-of-plane modal bending moments makes the assessments clear and simple. The project aims at defining the appropriate range of the procedure, as verified by tests and finite element analyses, as well as developing design aids and worked examples (Bijlaard et al., 2010). Figure 1 shows one of the LTB test setups.

Fig. 1. Lateral buckling test. (Photo courtesy of Professor Markus Feldmann)

The ultimate objective is to propose improved LTB rules in Eurocode 3.

Assessment of Structures with Welding Discontinuities: Professor Markus Feldmann is the director of this project and the primary researcher is Björn Eichler. The project is sponsored by the German council of steel construction, along with the Federal Ministry of Economics.

Design specifications and structural welding codes require full penetration welds for complete butt joints. This will sometimes lead to time-consuming and expensive repair work for the steel fabricator whenever the welds are produced with root gaps, as illustrated in Figure 2. A classification method for the assessment of such partial penetration details is still missing. Recently, a fitness-for-purpose strategy has been developed, primarily based on an accurate detection of the root gaps by nondestructive testing methods and then by a fracture mechanics solution in order to provide for the structural reliability of a welded steel member or joint (Feldmann et al., 2009).

Using this approach, a weld can be assessed in terms of its actual safety rather than having it be rejected due to insufficient penetration according to the conventional codes. The method uses a fracture mechanics safety assessment for a particular accidental scenario that includes extremely low temperatures, the presence of a root gap that is interpreted as a crack-like flaw, the presence of nominal stresses, and material properties as given in the governing material standards.

The results provide for sufficient bearing capacities for monotonic as well as cyclic loading. This can be verified for partial penetration in cross- and T-joints and also for butt joints for full penetration.

Toughness Requirements for Plastic Design with Structural Steel: Professor Markus Feldmann is the director for this project. The principal researchers are Dirk Schäfer and Björn Eichler. The project has been sponsored by the Commission of the European Union through the Research Fund for Coal and Steel (EU-RFCS).

The design criteria in Eurocode 3 (ECS, 2005), like those of all other structural steel design specifications in the world, are based on ductile material behavior. However, no mechanics-based criterion for the choice of a steel grade with sufficient toughness on the upper shelf of the toughness-temperature-diagram is available. This is particularly important for plastic design of structures with low-temperature service conditions.

Specifically, for the case of a cleavage fracture, the lower shelf of the toughness-temperature-diagram is relevant. A fracture mechanics assessment method has been developed and implemented to facilitate the choice of steel. However, considering the pure upper-shelf behavior, the method is not sufficient for practical purposes.

The European research project PLASTOTOUGH aims at developing an upper-shelf criterion for the choice of steel material for plastic design at low temperatures. Two approaches have been used: (1) a fracture mechanics solution is validated for monotonic loading, and (2) an approach based on damage mechanics has been developed for cyclic loading situations (Bleck et al., 2009). The damage mechanics solution is based on an extended von Mises yield criterion. This considers the formation, growth and coalescence of voids at the hot spot of plastic strain in the state of ductile fracture, with relation to damage curves that indicate crack initiation. Physical testing has demonstrated that the local ductility demands can be determined. Further, the results show that the strain requirements of global plastic rotations as well as of local strain demands can be verified, using both the fracture mechanics and the damage mechanics models.

As is well known by seismic researchers, in the case of seismic events a structure must provide appropriate deformation capacity. It can be shown that the cracking associated with ultra-low-cycle fatigue is not relevant for buildings, as long as the behavior is determined using reasonable limits

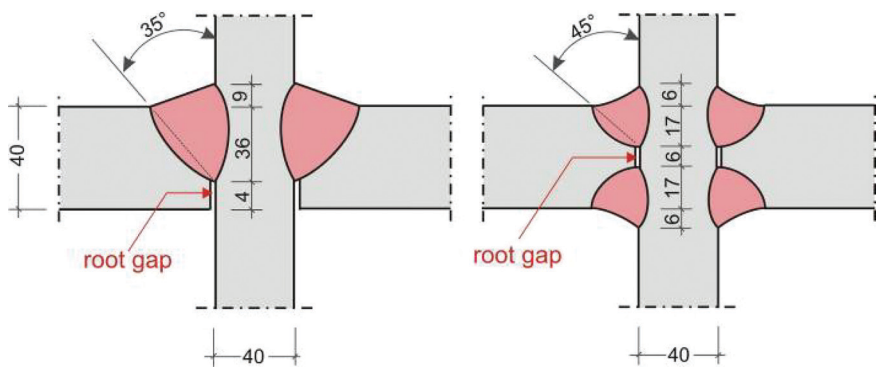

Fig. 2. Butt welds with root gaps (dimensions in mm).
(Figure courtesy of Professor Markus Feldmann)

for inter-story drift. For seismic issues these material performance investigations demonstrate that an elevated level of toughness is an appropriate solution (Feldmann et al., 2011a).

Composite Bridges with Integral Abutments: Professor Markus Feldmann is the director for this project. The principal researchers are Daniel Pak and Johannes Naumes. The project has been sponsored by the Commission of the European Union through the Research Fund for Coal and Steel (EU-RFCS).

The Institute of Steel Construction at Aachen has led the European project INTAB that aims at developing and promoting the integral abutments in composite bridge construction. It is one of the multi-institution, multicountry projects of the European Union, through the joint efforts of the Luleå University of Technology (Sweden), the University of Coimbra (Portugal), the University of Liège (Belgium) and the steel companies Arcelor (Luxembourg) and SSF (Germany).

Bridges with integral abutments are characterized by two unique features. First, the superstructure is fully fixed to the abutment structure, such that end moments are created that counteract the moments in the span, creating a bridge with relatively shallow members. Second, expensive expansion joints can be avoided.

As illustrated in Figure 3, the abutments are rigidly connected to the superstructure of integral bridges. The piles are not only loaded by vertical forces, but also by shear forces and moments as well as by forced displacements and rotations. The magnitude of these forces depends on a number of parameters, such as the stiffness of the soil, the stiffness of the superstructure, the stiffness of the piles and the length of the superstructure.

The interaction among the pile, the abutment and the girder is particularly important for the design of the piles. Rigid connections transfer all forces and displacements into the piles. Although these types of connections are generally preferred, the rigidity of the abutment and pile configuration, along with the soil interaction, is often unclear. Different approaches have been developed for considering the moment and force distributions in the abutment and the girder span, along with the effects of the continuous support of the soil behind the steel sheet pile and the low cycle resistance and response of the superstructure (Feldmann et al., 2011b).

Development of Innovative Steel-Glass Structures for Architectural and Structural Applications: This project was reported in the *Current Steel Structures Research* paper published in the first quarter 2012 issue of *Engineering Journal*. It is part of a larger-scale development of steel and glass structures. The lead research institution is RWTH Aachen; the research work presented in the earlier *Engineering Journal* issue was conducted at the Czech Technical University in Prague, the Czech Republic.

SOME CURRENT RESEARCH WORK AT THE FEDERAL UNIVERSITY OF RIO DE JANEIRO IN BRAZIL

The Federal University of Rio de Janeiro (FURJ) is the leading university in Brazil and a premier international university, with a broad program in all areas of civil engineering. The department of civil engineering has a large student population and a number of research activities, of which one of the most important areas is steel construction in all forms. Professor Eduardo Batista is the head of the

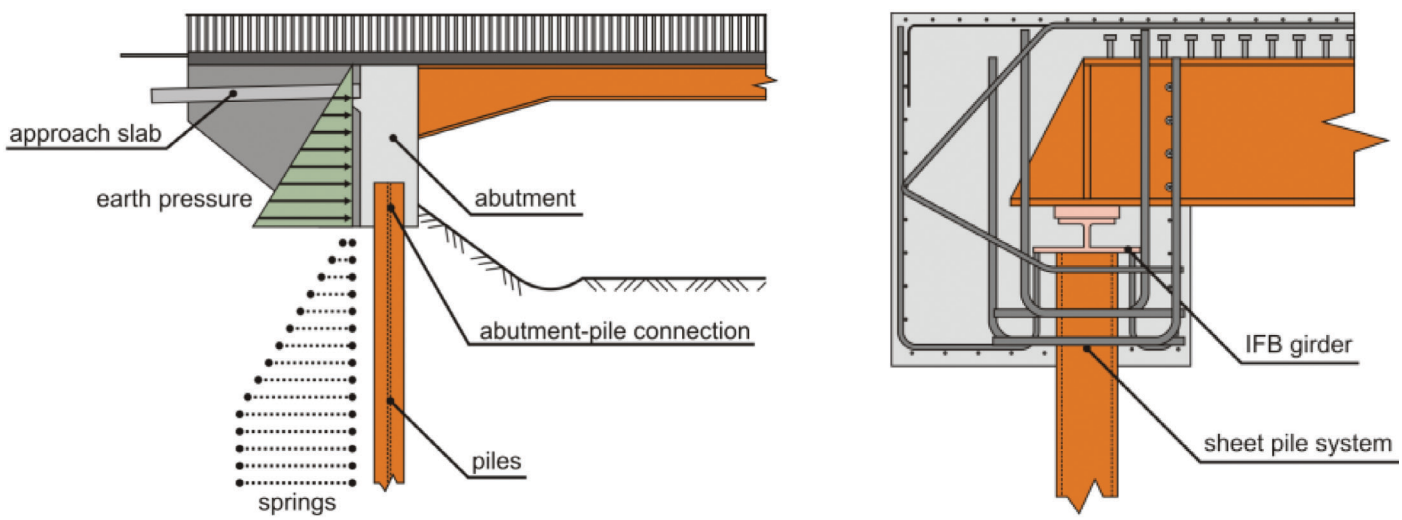

Fig. 3. Typical details of the integral abutment for a bridge. (Figure courtesy of Professor Markus Feldmann)

structural steel group; he and his colleagues are primary members of the Brazilian steel design code development work. They have published a number of significant papers in international journals and participate actively in workshops and conferences. Because of the robust Brazilian economy, the research and educational focus of the university is highly likely to make it an increasingly important institution in South America.

While a number of research projects are being conducted at FURJ, the following discussions will touch upon key efforts in three of the most active areas.

Cold-Formed Steel Construction: Cold-formed steel members in Brazil are primarily used for simple and small structural applications, such as in residential construction. Such elements are also used extensively for roofing and rack systems. The major benefits of cold-formed construction are derived from custom-made structural systems, as has typically been the case in North America and Europe. For emerging markets like those of many countries in South America, significant benefits are realized, especially for residential and small industrial applications.

As is recognized in design code applications, the complex structural behavior of thin-walled open sections is primarily dependent on torsional behavior and related stability phenomena. In particular, the interaction among the various buckling modes gives rise to limit states that are not found in hot-rolled steel members. The research activities at FURJ, therefore, aim to develop solutions for the following cold-formed member response characteristics:

1. Buckling behavior and nonlinear post buckling and buckling mode interaction.

2. Member strength, including for beams, columns, beam columns and trussed systems.

Fig. 4. Cold-formed trussed beam under full-scale load test (beam span 20 m = 67 ft). (Photo courtesy of Professor Eduardo Batista)

3. Design rules and procedures for practical design (Batista, 2009, 2010).

4. Development of suitable criteria for national design codes.

The FURJ researchers and the university interact aggressively with industry to address practical needs and applications. For example, rack systems and lightweight solutions for large-span roofing systems have been studied extensively. A project example is shown in Figure 4, where a trussed beam from a family of standard cold-formed structures was evaluated by numerical analyses and full-scale tests in order to assess its behavior under service loads and to identify the collapse mechanism and the eccentricity effects in the connections.

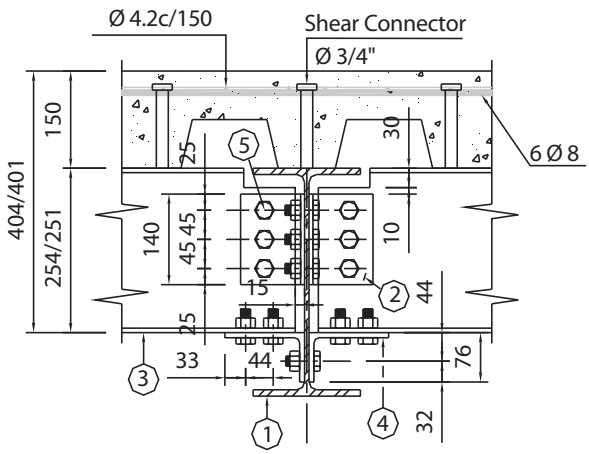

Fig. 5. Details of the semi-rigid beam-to-girder connection (dimensions in mm). (Drawing courtesy of Professor Eduardo Batista)

Performance of Steel-Concrete Composite Structures: Composite construction is now used extensively in Brazil, particularly for shopping malls and similar long-span systems, multi-story parking structures, and commercial high-rise buildings. Design and fabrication of suitable connections effectively determine the success of each project. The composite construction research at FURJ has therefore focused on beam-to-column connections, including the semi-rigid response characteristics (Oliveira and Batista, 2009). The projects have focused on the composite semi-rigid connections because such details offer potential cost savings and improved structural performance. With this background, it was decided to emphasize the semi-continuous floor system concept.

The research work was conducted in two steps: (1) test the connection itself through a series of individual full-scale tests and (2) test the beam-to-girder connection in a composite floor system. Figure 5 shows the details of the composite connection. The results were used to develop a proposed design method in a case study for an existing parking structure, concluding that it would provide significant economies for the project. Figure 6a shows the overall testing assembly, and Figure 6b provides a close-up view of the connection.

Behavior of Steel and Composite Structures under Fire Conditions: Professor Alexandre Landesmann is the director of this project. The focus is on thermo-mechanical performance of structures under high temperatures and fire conditions. Analyses are performed on the basis of a transient

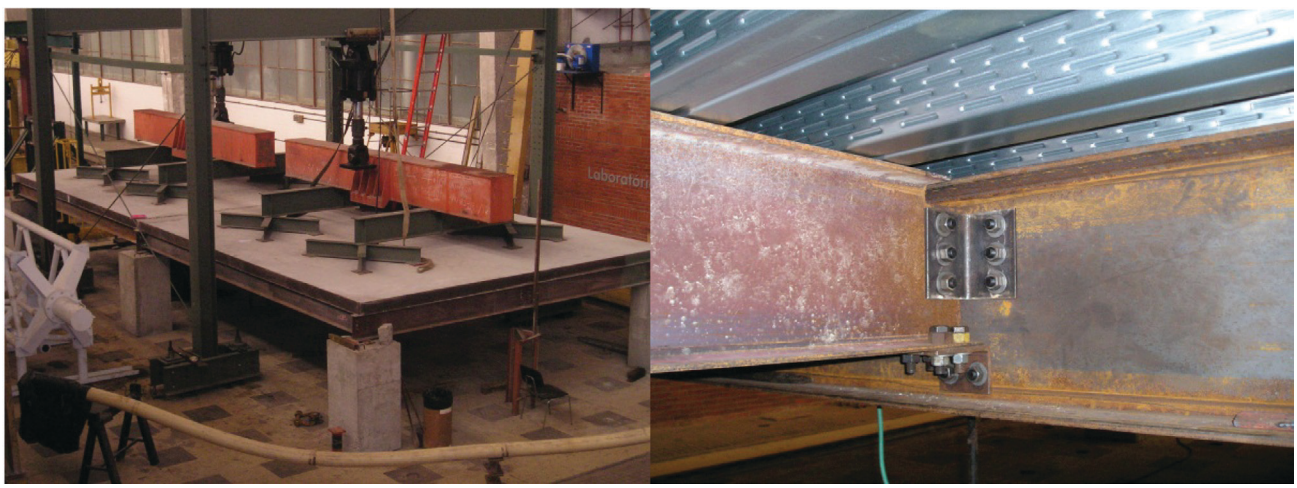

(a) *(b)*

Fig. 6. Full-scale testing of a semi-continuous floor system and one of the connections. (Photo courtesy of Professor Eduardo Batista)

heat-transfer model, which takes into account the properties of heated materials and simulates the inelastic behavior of steel and composite structures subjected to fire. The method of analysis also allows for different steel (insulated or not) and composite configurations (Landesmann, 2012).

The studies have now been expanded to include finite element analysis of the distortional post-buckling behavior, the ultimate strength and the design of cold-formed steel-lipped channel and rack-section columns subjected to various (uniform) temperature distributions. Figure 7 gives results for the von Mises stress distributions at the distortional collapse of 65-ksi yield stress steel columns and subjected to four different temperatures.

The failure load data gathered from the numerical analysis are used to carry out preliminary assessments of the applicability of the direct strength method (DSM) to estimate the load-carrying capacity of columns failing in distortional buckling under fire conditions (Landesmann and Camotim, 2010).

SOME CURRENT RESEARCH WORK AT THE UNIVERSITY OF CHILE IN SANTIAGO, CHILE

The University of Chile is one of the premier institutions in that country, with excellent contributions to the state of the art of steel structures, in particular as related to the seismic performance of industrial structures. The Chilean code for the seismic design of such structures is excellent and one of the very few in the world that addresses their unique considerations and demands (INN, 2003).

Steel construction in Chile is significantly complicated by the fact that the country has no steel mills that produce hot-rolled wide-flange shapes; even much of the plate steel has to be imported. As a result, the engineering profession has to use welded built-up shapes. With a small number of steel fabricators, the engineering talent is very broad and solid, and the fabricating equipment (especially for welding) is first class. The quality of steel construction is therefore generally very good, but material supply problems and costs will vary a great deal in response to international market conditions. Design and fabrication of steel structures in Chile can offer real challenges.

Double Split Tee Moment Connections: The director of this project is Professor Ricardo Herrera Mardones. Following the investigation prompted by the failures of steel structures after the 1994 Northridge earthquake, several new connections and improved connection details were proposed, and many more have been developed in recent years. Among them, the double split tee (DST) connection has been prequalified for use in steel seismic resistant construction.

Significant research has been conducted on the behavior of the connection and the tee-stub, providing models and design procedures that have been incorporated by various design codes. However, most of the research has been carried out on tee-stubs cut from hot-rolled wide flange sections.

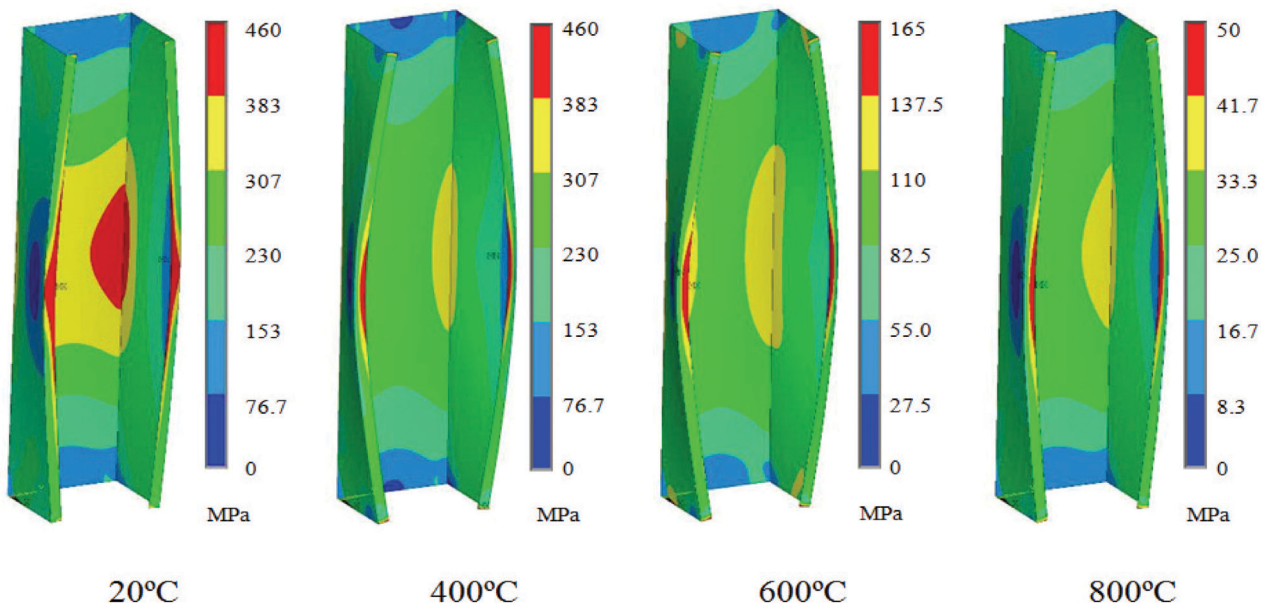

Fig. 7. Von Mises stress distributions for distortional buckling of columns at different temperatures. (Drawing courtesy of Professor Alexandre Landesmann)

Because welded tee-stubs have the advantage of improved material utilization and freedom of sizing, as compared to hot-rolled tee-stubs, and because Chile has no steel mills, the use of the welded DST was a natural consequence.

The proposed project will conduct analytical and experimental studies on the behavior of welded tee-stubs subjected to cyclic loading through the stem. The objectives of these studies include determining the limit states that control the behavior of welded tee-stubs, increasing the database of tests for these components, and evaluating the applicability of current design recommendations and models to welded tee-stub moment connections. To achieve these aims, finite element models of welded tee shapes will be calibrated and subjected to cyclic loading, and representative configurations will be tested under cyclic loading to simulate the conditions for a double welded tee moment connection. Simplified models and design recommendations will then be used for the design of double split tee connections.

It is expected that this project will provide designers with information to analyze and design structural systems with DWT connections and to generate data to prequalify the connections for use in seismic resistant design.

ACKNOWLEDGMENTS

Significant assistance has been provided by Professor Markus Feldmann of RWTH Aachen; Dr. Klaus Weynand of Feldmann + Weynand, Aachen, Germany; Professor Eduardo Batista and Professor Alexandre Landesmann of the Federal University of Rio de Janeiro in Brazil; Professor Carlos Aguirre of the Technical University "Federico Santa María" in Valparaíso, Chile; and Professor Ricardo Herrera of the University of Chile in Santiago, Chile. Their efforts are sincerely appreciated.

REFERENCES

Batista, E.M. (2009), "Local-Global Buckling Interaction Procedures for the Design of Cold-Formed Columns: Effective Width and Direct Method Integrated Approach," *Thin-Walled Structures*, Vol. 47, pp. 1218–1231.

Batista, E.M. (2010), "Effective Section Method: a General Direct Method for the Design of Steel Cold-Formed Members under Local-Global Buckling Interaction," *Thin-Walled Structures*, Vol. 48, pp. 345–356.

Bijlaard, F.S.K., Feldmann, M., Naumes, J., and Sedlacek, G. (2010), "The General Method for Assessing the Out-of-Plane Stability of Structural Members and Frames and Comparison with Alternative Rules in EN 1993—Eurocode 3—Part 1-1," *Steel Construction*, Vol. 1, pp. 19–33.

Bleck, W., Dahl, W., Nonn, A., Amlung, L., Feldmann, M., Tschickardt, D. and Eichler, B. (2009), "Numerical and Experimental Analyses of Damage Behaviour of Steel Moment Connection," *Engineering Fracture Mechanics*, Vol. 76, No. 10, pp. 1531–1547.

European Committee for Standardization (ECS) (2005), *Eurocode 3: Design of Steel Structures—Part 1-1: General Rules and Rules for Buildings*, Standard No. EN 1993-1-1, ECS, Brussels, Belgium.

Feldmann, M., Eichler, B. and Höhler, S. (2009), "A Method to Assess Root Gaps in Welded Seams of T- and Cross Joints," *Stahlbau*, Vol 78, No. 4, pp. 243–252 (*in German*).

Feldmann, M., Eichler, B., Schäfer, D., Sedlacek, G., Vayas, I., Karlos, V. and Spiliopoulos, A. (2011a), "Toughness Requirements for Plastic Design with Structural Steel," *Steel Construction*, Vol. 4, No. 2, pp. 94–113.

Feldmann, M., Pak, D., Hechler, O. and Martin, P.O. (2011b), "A Methodology for Modeling the Integral Abutment Behaviour of Non-Symmetrically Loaded Bridges," *Structural Engineering International*, Vol. 3, pp. 311–319.

Instituto Nacional de Normalizacion (INN) (2003), *Earthquake-Resistant Design of Industrial Structures and Facilities*, INN Standard NCh 2369-2003, Santiago, Chile (*in Spanish*).

Landesmann, A. and Camotim, D. (2010), "Distortional Failure and Design of Cold-Formed Steel Lipped Channel Columns under Fire Conditions," *Proceedings of SSRC Annual Stability Conference*, Orlando, Florida, pp. 505–532.

Landesmann, A. (2012), "Refined Plastic-Hinge Model for Analysis of Steel-Concrete Structures Exposed to Fire," *Journal of Constructional Steel Research*, Vol. 71-1, pp. 202–209.

Oliveira, T.J. and Batista, E.M. (2009), "Modelling Beam-to-Girder Semi-Rigid Composite Connection with Angles, Including the Effects of Concrete in Tension," *Engineering Structures*, Vol. 31, pp. 1865–1879.